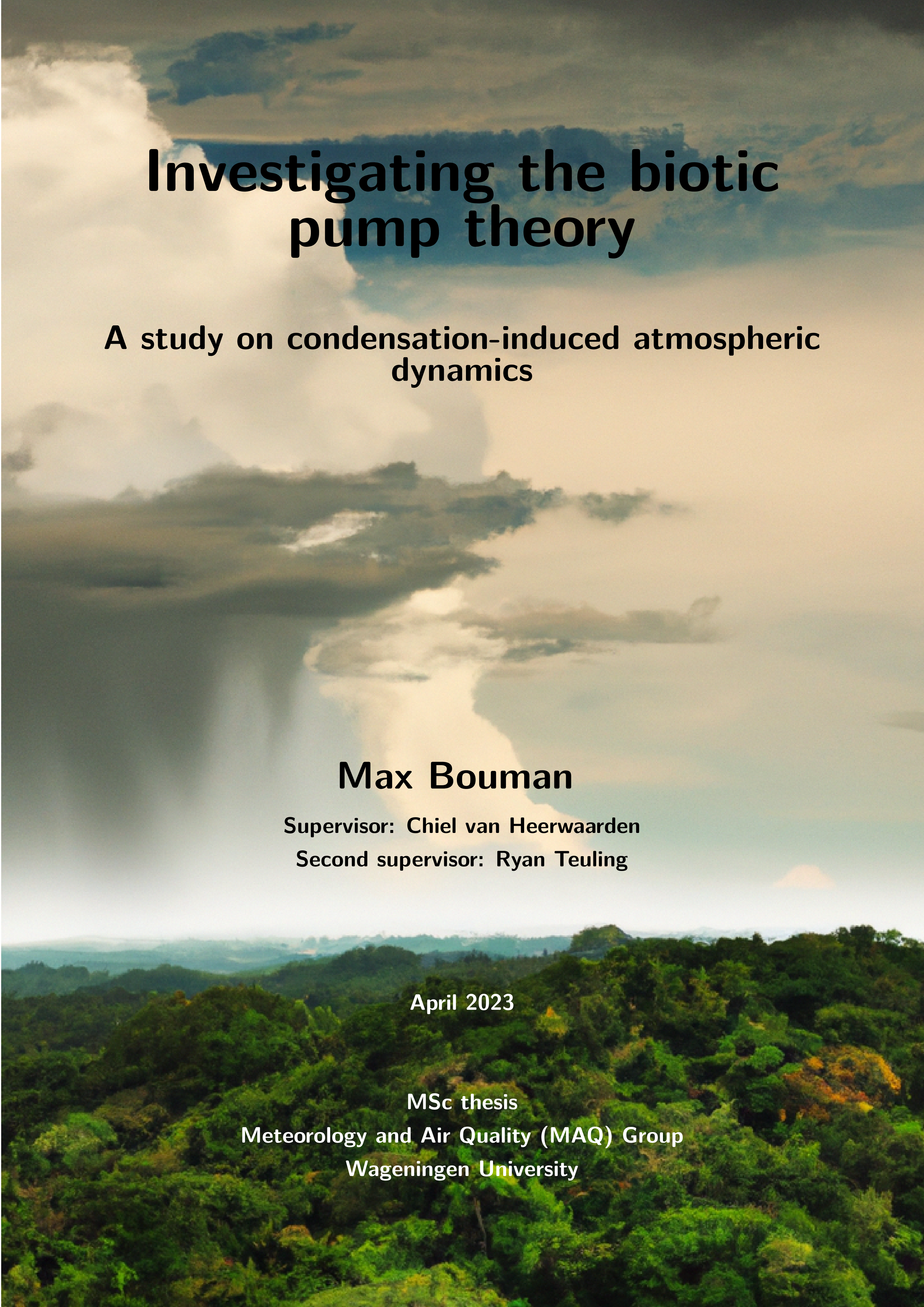

# Investigating the biotic pump theory

## A study on condensation-induced atmospheric dynamics


**Max Bouman**

Supervisor: Chiel van Heerwaarden

Second supervisor: Ryan Teuling


April 2023


MSc thesis

Meteorology and Air Quality (MAQ) Group

Wageningen University

# Abstract

The biotic pump theory links the phase change of water vapor to atmospheric pressure and dynamics. In essence, the theory describes how vegetation controls and regulates the amount of water vapor that enters the atmosphere and the subsequent rate of condensation. Due to the high leaf area index of forests, the evaporation rate over land can exceed the evaporation rate over the ocean resulting in more water vapor availability to condensate over land. The theory is controversial, because of the claim made by the authors of the biotic pump theory, that this condensation results in low pressure systems in the lower atmosphere. As a result, advection of moist air occurs from the oceans towards the continents, leading to even more precipitation over the continents. If true, the biotic pump theory could change our view on the role of vegetation in the water cycle and climate system and especially on the ongoing deforestation in regions such as the Amazon. To substantiate this, the theory builds on the concept of condensation-induced atmospheric dynamics. Condensation affects atmospheric pressure in two distinct ways: through both latent heating and mass removal. It is commonly accepted in the scientific community that the latent heating associated with condensation dominates over the effect of mass removal. By using the concept of condensation-induced atmospheric dynamics, the authors of the biotic pump theory came up with a theoretical condensation experiment to show that latent heating is in fact not dominant and that the role of mass removal in atmospheric dynamics is overlooked. In this research, the claims made by the authors of the biotic pump theory on the condensation-induced atmospheric dynamics are investigated. This is done through a detailed analysis of the steps of the theoretical condensation experiment by Makarieva et al. (2013) and by comparing it to another theoretical condensation experiment conducted by Spengler et al. (2011), who indeed found that there is a latent heating dominance associated with condensation. The results presented in this research suggest that the difference in results and conclusions based on the two experiments are not due to incorrect physical assumptions, but due to the different setup of the experiments. Especially, the amount of water vapor being condensed during the two experiments differs significantly. The amount of condensate ranges from 105 to 320 mm in the study by Makarieva et al. (2013) and is equal to 0.2 mm in the study by Spengler et al. (2011). By adjusting the experiment by Makarieva et al. (2013), in order to condense 0.2 mm of water vapor, and with the help of the relative pressure difference it is shown that both experiments yield similar results and that there is a latent heating dominance associated with condensation. Furthermore, the time scales associated with the pressure differences found by Makarieva et al. (2013) are discussed. Although the results show that mass removal can lower atmospheric pressure, it is unlikely that condensation is the main driver of atmospheric dynamics instead of differential heating based on this research. Overall, this study contributes to a better understanding of the controversy that is accompanied with the biotic pump theory and the condensation-induced atmospheric dynamics on which the theory builds.

# Contents

# 1 | Introduction

In this chapter, the background information for this research is provided. Forests are of key importance for the biotic pump theory. In **section 1.1**, the role of forests in the climate system is discussed and especially the effect of deforestation on precipitation is highlighted. **Sections 1.2** and **1.3** introduce the biotic pump theory and the condensation-induced atmospheric dynamics on which the theory is built respectively as well as pointing out the associated controversy. The last section of this chapter, **section 1.4**, provides insights in the ongoing debate that results from the complexity of the system of interest, from which the aim and research questions of this research naturally follow.

## 1.1 Deforestation & precipitation

Forests play an important role in Earth's climate system as they are a key component in the carbon and hydrological cycle and therefore provide opportunities to mitigate climate change (Bonan, 2008). To keep global warming limited to 1.5-2°C, models show that improved forest management, afforestation, reforestation and preventing deforestation are amongst the most important land based climate mitigation methods (IPCC, 2022). To better understand the role of forests in the climate system, a recent modelling study by Portmann et al. (2022) looked into the effects of restoring or removing all preindustrial vegetation cover. They found that restoring forest at a global scale would lead to profound changes in the atmospheric circulation (weakening and poleward shift of the Northern mid-latitude circulation and affecting the strength of the Hadley cell) as well as the ocean circulation (slowing down the Atlantic meridional overturning circulation). These changes in both atmosphere and ocean circulation have a global effect on precipitation patterns, temperature, clouds and surface wind patterns. The importance of forests in the climate system have thus been established. Yet, deforestation occurs worldwide at a high rate (Hansen et al., 2013), which results in a wide variety in both small and large scale consequences for both temperature and precipitation (Chambers and Artaxo, 2017; Lawrence and Vandecar, 2015).

Small scale deforestation in the tropics (length scale <200 km), resulting in heterogeneous land cover (mix of forest and pasture patches), can increase shallow clouds and precipitation locally. This is due to the increased sensible heat flux over pasture patches and thus thermal lifting, which generates atmospheric convection and the formation on clouds (Garcia-Carreras and Parker, 2011; Wang et al., 2009). However, small scale deforestation in boreal and temperate regions can decrease convective cloud formation due to differences in albedo, friction and biogeochemical processes (such as the release of BVOCs) as pointed out by Teuling et al. (2017). The effect of small scale deforestation on precipitation thus depends on the climate region of interest, which is supported by the recent observational study conducted by Xu et al. (2022) using satellite data, showing that forest cover loss led to cloud increase in the Amazon, Indonesia and Southeast US, but a reduction in clouds over East Siberia. Large scale deforestation (length scale >200 km) on the other hand is said to lead to a decrease of total precipitation as a result of both changes in boundary layer dynamics (i.e. decreasing surface roughness length and increasing albedo) and changes in the precipitation recycling due to decreasing evapotranspiration (less transpiration and canopy interception) (Devaraju et al., 2015; D'Almeida et al., 2007).

This scale dependency for the relation between deforestation and precipitation was also found in a very recent study conducted by Smith et al. (2023), who used satellite, station-based and reanalysis datasets to assess the precipitation decline across the tropics for various spatial scales during the time period 2003-2017. Their findings indeed show that the effect of deforestation on precipitation increases at larger scales and they estimated that precipitation will on average decline with 8-10% between 2015 and 2100 as a consequence of ongoing deforestation. In addition, they use linear scaling to estimate a decline of 10-20% in precipitation in case of complete deforestation. Attempts to estimate the effect of complete deforestation of tropical rain forests on precipitation have been made by numerous studies for various regions and using different methods. Estimates for the local precipitation decline in case of complete deforestation in the Congo basin range between 18 and 50 % (Spracklen et al., 2018; Duku and Hein, 2021), whereas in the Amazon Basin estimates range between 16 and 70% (Spracklen and Garcia-Carreras, 2015; Baudena et al., 2021; Lejeune et al., 2015; Medvigy et al., 2011; Leite-Filho et al., 2021). The spread in these estimates is partly due to the varying methods (e.g. numerical vs observational), but mainly due to including linear and nonlinear responses of the climate system as pointed out by each of these studies.

## 1.2 The biotic pump theory

Already 15 years ago, a paper was published in which a novel theory called the biotic pump of atmospheric moisture was proposed by Makarieva and Gorshkov (2007). This theory relates the phase transitions of water vapor in the atmosphere to atmospheric pressure and dynamics and results in a circulation that brings moist air from the oceans towards the continent. According to the authors, the processes that result in the biotic pump circulation are previously overlooked or wrongly assumed to be small. They claim that condensation, the engine of the biotic pump, might be one of the main drivers of atmospheric dynamics and to correctly quantify the effects of deforestation on precipitation, these effects have to be included in Global Circulation Models (GCM's). Their estimates suggest that further deforestation of the Amazon region could lead to a decrease of 80% in precipitation as a result of the seizing of the biotic pump. The same authors published a paper 5 years later, in which the condensation-induced dynamics (the engine of the biotic pump) were explained in depth (Makarieva et al., 2013). Both papers triggered a lot of discussion and until now the theory remains under debate.

One of the main reasons for the discussion is the claim that condensation is the main driver of global atmospheric circulation instead of differential heating, which is the commonly accepted driver of atmospheric dynamics (Gill, 1982). Differential heating is the difference between incoming solar radiation between the poles and the equator, which results in a temperature gradient. Together with the concept of buoyancy (warm air is lighter than cold air and will therefore rise whereas cold air sinks), a circulation pattern arises: warm air rises at the tropics and sinks again at the poles. Due to the rotation of the Earth, there are three different atmospheric circulation cells: the Hadley cell, Ferrel cell and the Polar cell. Before diving deeper into the controversy surrounding the biotic pump theory and the condensation-induced dynamics on which the theory is build, the concept of hydrostatic equilibrium has to be introduced. For large scale atmospheric dynamics, we can assume that the atmosphere is in approximate hydrostatic equilibrium (Gill, 1982). This equilibrium (equation 1.1) describes the distribution of air molecules in the atmosphere as a result of the balance between the gravitational force exerted by the Earth on molecules in the atmosphere and the collisions between molecules.

$$-\frac{dp}{dz} = \rho g \tag{1.1}$$

Here $p$ is the atmospheric pressure, $z$ is the height of the atmosphere, $\rho$ is the density of the air and $g$ is the gravitational constant.

## 1.3 Condensation-induced atmospheric dynamics

Condensation affects the hydrostatic equilibrium and thus atmospheric pressure which was already pointed out in a study by Bannon (1995), who investigated the hydrostatic adjustment of air in a one-dimensional column after heating an air layer. The heating of an air layer can be linked to the latent heat being released upon condensation, which increases pressure within the layer being heated. This in turn results in an upward motion of the heated air, but it does not affect the layer underneath the heated layer. In an additional study, Bannon et al. (2006) showed that there is a second mechanism that influences atmospheric pressure: mass removal. Due to condensation, the amount of water vapor molecules in the atmosphere decreases, after which hydrostatic adjustment occurs. Mass removal lowers the atmospheric pressure within and below the layer in which condensation occurs. So there are two mechanisms associated with condensation that affect atmospheric pressure, but in opposite ways.

The controversy of the biotic pump theory and the condensation-induced dynamics not only resides in the claim that it is condensation that drives atmospheric dynamics instead of differential heating, but also in the claim that it is the mass removal mechanism that drives the atmospheric circulation. This once again contradicts the conventional wisdom that the effect of latent heating dominates over the effect of mass removal. This was found in a study conducted by Spengler et al. (2011) who built further on the studies by Bannon (1995); Bannon et al. (2006). In order for the biotic pump to work, condensation must lead to a sufficient pressure decrease through the mass removal mechanism in the lower atmosphere. This is illustrated in figure 1.1.

The biotic pump circulation as described in the paper by Makarieva and Gorshkov (2007) is a self-sustaining

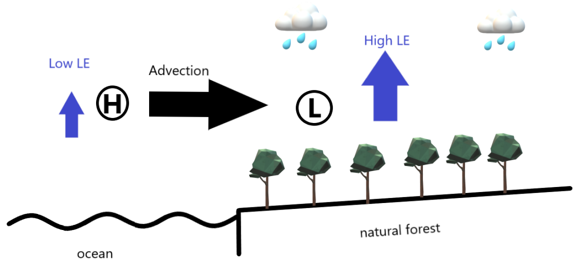


Figure 1.1: *The evaporation rate over natural forests can be higher than over open water bodies. This provides large amounts of water vapor to the atmosphere over the continents, which can result in condensation. According to the paper by Makarieva et al. (2013), condensation results in low pressure systems in the lower atmosphere. Due to the low pressure system, moist air is advected from the ocean towards the continents.*

circulation. Natural forests can maintain higher evaporation rates than open water bodies, such as the ocean, through their high Leaf Area Index (LAI). Due to the high evaporation rate, there is a lot of water vapor available to condensate. Once condensation occurs and low pressure systems start to form in the lower atmosphere, moist air is advected from the ocean towards the continent. As a result there is even more moisture available for condensation over the continent and so on. However, if the effect of latent heat release dominates over the effect of mass removal (as concluded by Spengler et al. (2011)), the circulation would occur in the exact opposite way. The resulting circulation is shown in figure 1.2.

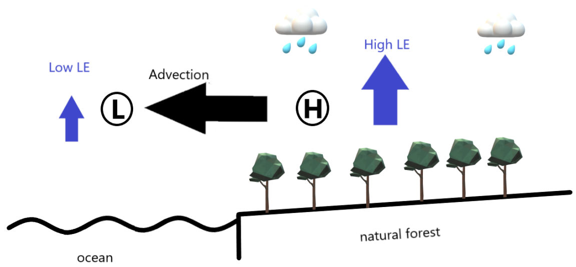


Figure 1.2: *This figure is similar to figure 1.1, except for the fact that here it is assumed that condensation leads to high pressure systems. As a result air is advected from the continents towards the oceans.*

In that case, the high evaporation rate over natural forest would still lead to condensation. However, condensation would lead to high pressure areas over the continent. As a result, air would be advected towards the ocean. Note that the latent heating dominance would not necessarily suggest that this circulation occurs. As mentioned before, it is commonly believed that differential heating is the driver of atmospheric dynamics and that the effects of condensation (latent heat release and mass removal) only play a secondary role in driving the global atmospheric circulation.

## 1.4 The ongoing debate

One of the reason why this theory is still under debate, is that the atmosphere is a complex system where the variables of interest for this research are interlinked through the ideal gas law (equation 1.2).

$$p = \rho R T \tag{1.2}$$

Here $R$ is the universal gas constant and $T$ is the temperature of the air. This is further complicated when moist convection is considered instead of dry convection, because it interacts non-locally with other parts of the flow through radiative, gravity waves or microphysical (precipitation) processes (Stevens, 2005). Especially, moist atmospheric convection in the tropics is hard to model as it involves multiple scale interactions between convection, clouds, radiation and dynamics (Hu, 2020). Therefore, disentangling effects of specific processes is very difficult. Even though our understanding and representation of the climate system in climate models has improved significantly (IPCC, 2022), atmospheric convection is among the most important model limitations (Douville et al., 2021). This manifests itself in inaccurate modelled tropical precipitation amounts (Volodin et al., 2018; Li et al., 2020). The so-called 'double inter-tropical convergence zone (ITCZ)' is a good example of this, which is the occurrence of a double zonal band of precipitation in models located in the equatorial central Pacific that is not supported by observations leading to excessive modelled precipitation over much of the tropics (Lin, 2007). It has been a problem in the state of the art GCM's, from CMIP3 to CMIP5 and even now in the most recent CMIP6 models (Zhang et al., 2015; Tian and Dong, 2020). Convective parameterization is amongst the most important contributors to this problem and therefore has the most potential to reduce the modelled excessive amounts of precipitation (Zhang et al., 2019). According to the authors of the biotic pump theory, it is the parameterization of convection and other processes in GCM's that conceal the effect of the biotic pump feedback mechanism. They argue that the parameterization schemes for convection and other processes do not fully account for the interactions between forests and atmospheric pressure and dynamics, which limits the model's ability to accurately represent the true behavior of the climate system and may lead to incomplete or biased predictions. As a result, the aforementioned estimates of the effect of deforestation on precipitation that are deducted from model results and linearly extrapolated observational studies, potentially (strongly) underestimate the effect of deforestation.

Besides the aforementioned complexity of the system, the resulting general circulation as shown in figure 1.1 is inconclusive for determining the validity of the biotic pump theory. That is because it is very similar to the circulation that occurs according to the differential heating theory. However, in a paper by Sheil (2018) some scenario's are discussed for which the biotic pump theory could be used to explain the circulation, but not the differential heating theory. An example is the 'cold Amazon paradox', which is the occurrence of landward blowing winds from the Atlantic ocean towards the Amazon region, even though the land is colder than the ocean. The reasoning in that paper is as follows: the evaporation rate over the Amazon exceeds the evaporation rate over the ocean leading to relatively lower pressure areas over land and thus landward blowing winds. Sheil (2018) acknowledges that there might be other explanations for this specific scenario, such as the mechanism described in Wright et al. (2017): shallow convection leads to accumulation of moisture in the lower atmosphere and destabilizes it, which preconditions the atmosphere for deep convection later on and thereby results in moisture convergence before the ITCZ arrives.

The biotic pump theory could have far reaching consequences through the described phase transitions of water vapor and the resulting influence on atmospheric pressure and dynamics (Makarieva and Gorshkov, 2007):

- Undermining the importance of differential heating.
- Change our view on the state of the art climate models and the possibly wrongly used parameterization.
- Reduce parameterization in GCM's and make them more physically based.
- Explain difficulties with modelling moist convection and precipitation in GCM's.
- Lead to higher than currently expected large-scale precipitation reductions due to deforestation in coastal regions.

The papers by Makarieva and Gorshkov (2007); Makarieva et al. (2013) were both published in a journal that allows open access interactive discussion forums, which means that the reviews are available for everyone to read. Multiple reviewers advised to reject the paper by Makarieva et al. (2013), but in the end the paper was published with the following comment from the the handling editor, Athanasios Nenes (Makarieva et al., 2011): *"The handling editor (and the executive committee) concluded to allow final publication of the manuscript in ACP, in order to facilitate further development of the presented arguments, which may lead to disproof or validation by the scientific community."*

Due to possibly far reaching consequences, it is of utmost importance that the reliability the biotic pump theory is established. Therefore, this research aims to contribute to disproving or validating the condensation-induced atmospheric dynamics on which the biotic pump theory is built by answering the following research questions:

1. What is the effect of condensation on pressure in an air column?
2. What are the assumptions made in the paper by Makarieva et al. (2013) that could explain the divergent conclusions, related to condensation effects on atmospheric pressure, from other research on this topic?
3. How large are the effects of these assumptions on the atmospheric pressure in an air column?

To answer these research questions, the theoretical condensation experiment presented in the paper by Makarieva et al. (2013) will be investigated and compared to the theoretical condensation experiment by Spengler et al. (2011). The setup of both condensation experiments, as well as some adjustments to be able to compare them, will be described in **chapter 2**. The results of the comparison will be presented and discussed in **chapters 3** and **4**, respectively, and the main conclusions of this research will be provided in **chapter 5**.

# 2 | Methods

In this chapter, the methods for modelling the condensation experiment are provided. These methods require a proper understanding of the condensation induced dynamics and therefore this chapter will also partly be a 'concept' chapter to accompany the used methods and provide the physical explanation behind the described methods.

The effect of condensation through mass removal and latent heat release on atmospheric (surface) pressure is the fundamental pillar of the biotic pump theory. Makarieva et al. (2013) came up with a theoretical experiment to quantify the effects of the two processes. As mentioned in the introduction, the main finding presented in the paper by Makarieva et al. (2013) based on the condensation experiment, is that there is no clear 'latent heating dominance'. This finding contradicts previous research and therefore the authors state that the effect of mass removal associated with condensation has a significant effect on atmospheric pressure and that it did not receive enough attention.

An important part of this research is to check the validity of the biotic pump theory and evaluate the claims made based on this experiment. To do so, the condensation experiment conducted by Makarieva et al. (2013) has been replicated to check all of the intermediate steps and get a better understanding of the condensation induced dynamics. For completeness of this report, the methods for the experiment conducted by Makarieva et al. (2013) are included in **section 2.1**, making this section similar to the one presented in the paper by Makarieva et al. (2013), sections 3.1-3.3.

As stated before, previous research, such as the work by Spengler et al. (2011) found that there is a clear latent heating dominance over mass removal effects associated with condensation. They also conducted a theoretical condensation experiment, but with a different method setup, from which such conclusions were drawn. In this research, the experiments by Makarieva et al. (2013) and Spengler et al. (2011) are compared to each other. The methods for the experiment by Spengler et al. (2011) are shortly touched upon in **section 2.2**. To be able to compare the two condensation experiments, some adjustment of the experiment by Makarieva et al. (2013) are needed. The methods for adjusting the experiment by Makarieva et al. (2013) are provided in **section 2.3**.

## 2.1 Replica experiment Makarieva et al. (2013)

An important aspect of the biotic pump theory and the condensation-induced atmospheric dynamics, is the difference between dry (non-condensable) and moist (condensable) air. This difference and its effect in a dynamic atmosphere is illustrated in the following experiment. The original experiment by Makarieva et al. (2013) consists of 4 steps, which are explained in **subsections 2.1.1 - 2.1.4**. **Section 2.1.5** provides the physical explanation about the scale heights being used in this theoretical condensation experiment.

### 2.1.1 Isothermal atmosphere

We start with two columns. One column that contains moist air, column A, and one column that contains dry air only, column B. Both columns start with the same surface pressure, $p_{s,A} = p_{s,B}$, the same surface temperature, $T_{s,A} = T_{s,B}$, and are isothermal i.e. $\frac{dT}{dz} = 0$. The water vapor in column A is saturated at the surface, but not saturated above the surface. The amount of water vapor being held in the atmosphere follows the Clausius-Clapeyron equation (eq. 2.1) and is therefore a function of temperature only.

$$\frac{dp_v}{p_v} = \zeta \frac{dT}{T}, \quad \zeta \equiv \frac{L}{RT} \tag{2.1}$$

In this equation, $p_v$ is the water vapor pressure, $T$ is the temperature, $L$ is the latent heat of vaporization and $R$ is the universal gas constant.

### 2.1.2 Temperature lapse rate

The next step is to apply temperature lapse rates to the air columns, which makes them non-isothermal. The moist adiabatic lapse rate ($\Gamma_m$, eq. 2.2) is applied to column A (containing the moist air).

$$\frac{dT_m}{dz} = \Gamma_m = \varphi \frac{T}{h}, \quad \varphi \equiv \mu \frac{1+\gamma\xi}{1+\gamma\mu\xi^2} \tag{2.2}$$

With:

$$\mu \equiv \frac{R}{c_p}, \quad \gamma \equiv \frac{p_v}{p}, \quad h \equiv \frac{RT}{Mg} \tag{2.3}$$

Here, $M$ is the molar mass of air, $c_p$ is the molar heat capacity at constant pressure and $g$ is the gravitational constant. The moist adiabatic lapse rate depends on the amount of water vapor in the atmosphere. From equations 2.2 and 2.3 it can be seen that there are 3 unknown variables ($T$, $p_v$ and $p$) involved in the calculation of the moist adiabatic lapse rate, for which we thus need at least 3 equations. Therefore, the Clausius-Clapeyron equation differentiated over z (equation 2.4) and the equation for hydrostatic equilibrium (equation 2.5) are added to this system of equations, as these equations govern the distribution of water vapor in the atmosphere.

$$\frac{dp_v}{dz} = -\frac{p_v}{h_v}, \quad h_v \equiv \frac{RT^2}{L\Gamma_m} \tag{2.4}$$

$$\frac{dp}{dz} = -\rho g = -\frac{p}{h} \tag{2.5}$$

To be able to solve these ODE's, initial parameter values are needed for $T$, $p_v$ and $p$. These values can be found in table 2.1. To keep consistent with the study by Makarieva et al. (2013), the same 3 surface temperatures are chosen (see the values underneath set 1, 2 and 3). The value for the surface pressure is identical for all 3 sets, because the surface pressure only depends on the amount of gas molecules in the atmospheric column and not on temperature. Note that the values underneath set 4 in table 2.1 belong to the adjusted experiment, which will be explained in section 2.3.

Table 2.1: *Initial parameter values needed to solve the set of ODE's for the moist adiabatic lapse rate. Set 1, 2 and 3 are used in the replica condensation experiment. Set 4 is used for the adjusted experiment (see section 2.3).*

| | set 1 | set 2 | set 3 | set 4 |
|---|---|---|---|---|
| $T_0$ (K) | 303 | 293 | 283 | 214 |
| $p_0$ (Pa) | 101325 | 101325 | 101325 | 101325 |
| $p_{v0}$ (Pa) | 4209 | 2317 | 1216 | 2.14 |

However, the value for the partial pressure of water vapor, $p_{v0}$, does depend on temperature according to the Clausius-Clapeyron equation. This value can be approximated by using the Arden-Buck approximation (equation 2.6).

$$\begin{gathered} p_v(T) = a\exp\left(\left(b - \frac{T}{c}\right)\left(\frac{T}{d+T}\right)\right), \quad with \\ a = 0.61121, \quad b = 18.678, \quad and \\ c = 234.5, \quad d = 0.61121 \end{gathered} \tag{2.6}$$

In this equation $p_v$ is in kPa and $T$ is in °C. Solving this set of equations allows to find a temperature profile for column A after a part of the water vapor in the column has condensed (and latent heat has been released) due to applying the moist adiabatic lapse rate and thus the subsequent temperature decrease.

The dry adiabatic lapse rate ($\Gamma_d$, eq. 2.7) is applied to column B (containing the dry air).

$$\frac{dT_d}{dz} = \Gamma_d = \frac{M_d g}{c_p} \tag{2.7}$$

Equation 2.7 shows that the dry adiabatic lapse rate does not depend on height. It has a constant value throughout the entire dry column. The temperature profile in the two columns can be determined by using equation 2.8.

$$T_{z,A} = T_s - \Gamma_m z, \quad T_{z,B} = T_s - \Gamma_d z \tag{2.8}$$

Due to the use of the two different adiabatic lapse rates (moist and dry) this theoretical condensation experiments, the effect of latent heat release is incorporated and can be quantified as the difference between the resulting pressure profiles.

### 2.1.3 Surface pressure perturbation

As mentioned in the previous section, surface pressure, $p_s$, only depends on the amount of gas molecules in the air column above it and not on the temperature profile of the air column. Due to the condensation that occurs in column A when the moist adiabatic lapse rate is applied, the amount of water vapor molecules (and thus the total amount of gas molecules) is reduced. Condensation does not occur in column B. As a result, the surface pressure in column A must be lower than the surface pressure in column B after applying the lapse rates, $p_{s,A} < p_{s,B}$, because they were exactly equal before applying the lapse rates. Equation 2.9 shows how the surface pressure perturbation, $\delta p_s$, that results from the reduction in gas molecules is calculated.

$$\delta p_s = p_v(T_s)\left(1 - \frac{h_{vs}}{h_{ns}}\right) \tag{2.9}$$

In this equation, $h_{vs}$ and $h_{ns}$ are the scale heights for the vertical distribution of saturated water vapor and the hydrostatic distribution of water vapor in an isothermal atmosphere respectively, evaluated at the surface. In the paper by Makarieva et al. (2013), these scale heights are defined as in equation 2.10.

$$h_{vs} = \frac{RT_s^2}{L\Gamma_s}, \quad h_{ns} = \frac{RT_s}{M_v g} \tag{2.10}$$

The scale height $h_{vs}$ can be obtained by differentiating both sides of equation 2.1 over $z$ (see equation 2.4) and by approximating $h_v(T(z)) = h_v(T_s)$. On the other hand, $h_{ns}$ is derived by substituting the ideal gas law of water vapor into the hydrostatic equilibrium of water vapor, resulting in equation 2.11.

$$\frac{dp_v}{dz} = -\frac{p_v}{h_n}, \quad h_n = \frac{RT}{M_v g} \tag{2.11}$$

In the isothermal atmosphere the temperature is constant with height, $T(z) = T_s$, and as a result $h_n = h_{ns}$. By substituting the right hand sides of the scale heights from equation 2.10 into equation 2.9, we find equation 2.12.

$$\delta p_s = p_v(T_s)\left(1 - \frac{M_v g T_s}{L\Gamma_s}\right) \tag{2.12}$$

This equation allows to calculate the surface pressure perturbation from known variables and constants.
The physical explanation of the scale heights is provided in subsection 2.1.5.

### 2.1.4 Comparing the two columns

The condensation that occurred due to applying the moist adiabatic lapse rate in column A has two distinct effects on the pressure in the column:

1. Latent heat is released during the condensation. As a result the pressure, $p(z)$, at any height in the column where condensation occurs increases due to the relation between temperature and pressure as described by the ideal gas law (equation 1.2).

2. The surface pressure declines due to the decrease of the total amount of gas molecules in the atmospheric column.

The effect of (1) latent heating is incorporated in the calculation of the moist adiabatic lapse rate and the temperature profile that results from it (equation 2.2 and 2.8) and the effect of (2) a decreasing amount of gas molecules in the atmospheric column can be determined with equation 2.12. Now that the two effects of condensation are quantified, we can compare the resulting pressure profiles, $p_A(z)$ and $p_B(z)$, to each other after an approximate hydrostatic equilibrium is established in the two columns (Equation 2.13 and 2.14).

$$p_A(z) = p_s\left(1 - \frac{\delta p_s}{p_s}\right)\exp\left\{-\int_0^z \frac{dz'}{h_A(z')}\right\} \tag{2.13}$$

$$p_B(z) = p_s \exp\left\{-\int_0^z \frac{dz'}{h_B(z')}\right\} \tag{2.14}$$

### 2.1.5 Physical explanation scale heights

In the previous sections, multiple scale heights were derived. The derived scale heights are: $h$ for the distribution of the air mixture as a whole in a non-isothermal atmosphere (equation 2.3), $h_v$ for the distribution of water vapor in a non-isothermal atmosphere (equation 2.4) and $h_n$ for the distribution of water vapor in an isothermal atmosphere (equation 2.11). These scale heights govern the distribution of water vapor in the atmosphere by dictating how fast the amount of molecules decrease with height. This can also be seen from the fact that the scale heights are present in the exponents of the equations for the pressure profile of column A and B (equation 2.13 and 2.14). Different scale heights in the exponents of these equations will result in a different pressure decrease with height.
The reason that these scale heights are obtained by differentiating two different equations over z is as follows. As explained in the paper by Makarieva and Gorshkov (2009), the distribution of water vapor is not only dependent on gravity, but also on temperature through condensation. This is how water vapor distinguishes itself from the 'dry' atmospheric gasses. If we would now assume that water vapor would behave as a 'dry' gas, meaning that it acts as a non-condensable gas, then the distribution of water vapor throughout the atmospheric columns would solely be determined by the hydrostatic equilibrium of the partial pressure of water vapor. The hydrostatic equilibrium of course also depends on the temperature through the density. By assuming a hypothetical temperature profile, where the temperature is constant with height and thus equal to the surface pressure, a background value of the water vapor distribution in the atmosphere is established. This background value for the water vapor distribution allows to compare against a physically correct scenario in which water vapor does depend on temperature through both condensation (Clausius-Clapeyron) and gravity (hydrostatic equilibrium). As the surface pressure, $p_s$, in the columns only depends on the amount of gas molecules in the atmospheric columns, the difference between the two scenarios regarding the surface pressure is the amount of water vapor that has condensed by applying the Clausius-Clapeyron equation. This means that the scale heights, $h_{vs}$ and $h_{ns}$, can be used to calculate the surface pressure perturbation as a result of condensation (equation 2.9).

## 2.2 Experiment Spengler et al. (2011)

In this research, the results of the paper by Spengler et al. (2011) are chosen to compare against the results found by Makarieva et al. (2013). There are a few reasons why this paper is chosen. Most importantly, both papers try to quantify the effect of latent heat release and mass removal, associated with condensation, on atmospheric pressure in a one-dimensional framework. The methods presented in the paper by Spengler et al. (2011) yield different results than the one by Makarieva et al. (2013). As a result, the conclusions of both papers contradict each other. The paper by Spengler et al. (2011) claims that the effect of latent heat release dominates over the effect of mass removal. On the other hand, the paper by Makarieva et al. (2013) states that the effect of mass removal dominates in the lower atmosphere and is overlooked due to incorrect assumptions. They even argue that mass removal is an important (if not the main) driver of atmospheric dynamics. In addition, the results presented in the paper by Spengler et al. (2011) seem to be commonly accepted by the scientific community, as it builds on previous research (Bannon, 1995; Bannon et al., 2006), whereas the study conducted by Makarieva et al. (2013) is a novel but controversial theory according to the reviews. Finally, the results of this paper are discussed in some of the reviews on the ACP open access interactive discussion forum of the paper by Makarieva et al. (2013).

For completeness of this research, a brief description of the methods used in the paper by Spengler et al. (2011) is provided. The description is not as detailed as for the condensation experiment by Makarieva et al. (2013), because the paper by Spengler et al. (2011) is mainly used to compare the results to the results found by Makarieva et al. (2013) instead of reproducing the methods to validate their result.

The study conducted by Spengler et al. (2011) includes the effects of mass removal and latent heat release associated with condensation in a similar way as in the study by Bannon et al. (2006) under the assumption that the atmosphere is in hydrostatic equilibrium. In addition, the effect of hydrometeors is included. To do so, the linearized one-dimensional momentum equations are used (equations 2.15, 2.16 and 2.17), which were also used in the paper by Bannon (1995).

$$\frac{\partial w'}{\partial t} = -\frac{1}{\overline{\rho}}\frac{\partial p'}{\partial z} - g\frac{\rho'}{\overline{\rho}} + F \tag{2.15}$$

$$\frac{\partial \rho'}{\partial t} = -\overline{\rho}\frac{\partial w'}{\partial z} - w'\frac{\partial \overline{\rho}}{\partial z} \tag{2.16}$$

$$\frac{\partial p'}{\partial t} = -\overline{\rho} g w' - \overline{p}\gamma\frac{\partial w'}{\partial z} \tag{2.17}$$

In order to solve this system of equations, the diagnostic equations are used (equations 2.18 and 2.19).

$$\frac{p'}{\overline{p}} = \frac{\rho'}{\overline{\rho}} + \frac{T'}{\overline{T}} \tag{2.18}$$

$$\frac{\theta'}{\overline{\theta}} = \frac{p'}{\gamma\overline{p}} - \frac{\rho'}{\overline{\rho}} \tag{2.19}$$

It is assumed that at $t = 0$, 0.2 $kg/m^2$ of water vapor is instantaneously converted to water droplets in the layer between 4 and 6 km (see equation 2.20).

$$m_w = \int_{z_1}^{z_2} \rho_v dz \tag{2.20}$$

Here, $m_w$ is the water vapor mass per unit area that is being condensed, $z_1 = 4$ km and $z_2 = 6$ km. An initial pressure perturbation is present before condensation occurs ($t < 0$). This initial pressure perturbation results from the comparison that is made between the case in which there is 0.2 $kg/m^2$ of water vapor in the atmosphere and a completely dry atmosphere. Water vapor is lighter than dry air with the initial pressure perturbation as a result. At $t = 0$, all of the water vapor condenses. Mass is removed from the system and latent heat is released. To calculate the effect of latent heating, equation 2.21 is used.

$$T_0' = -\frac{L_v\rho_0'}{c_v(\overline{\rho} - \rho_0') + c_w\rho_v} \approx -\frac{L_v\rho_0'}{c_v\overline{\rho}} \tag{2.21}$$

After condensation, the rain drops will accelerate due to the gravitational force until they reach their maximum velocity. However, this research will not focus on the effects of the rain drops on atmospheric pressure, but only on the initial state (described above) and the equilibrium state (described below).

The equilibrium state ($t \to \infty$) is reached when all rain drops have reached the surface and hydrostatic adjustment is achieved, bringing the system back in hydrostatic equilibrium. As in Bannon (1995), a conserved quantity (equation 2.22) is integrated from $t = 0$ to $t \to \infty$ to find the hydrostatic pressure at $t \to \infty$.

$$\left[\left(\overline{\rho}\frac{\frac{p'}{\gamma\overline{p}} - \frac{\rho'}{\overline{\rho}}}{\frac{\overline{p}_z}{\gamma\overline{p}} - \frac{\overline{\rho}_z}{\overline{\rho}}}\right)_z - \rho'\right]_t = 0 \tag{2.22}$$

By assuming that there is no vertical displacement at the lower boundary, a decrease in surface pressure is prescribed equivalent to the mass of water vapor being removed from the atmospheric column.

The equilibrium state of the pressure profile in the paper by Spengler et al. (2011) is found through an analytical as well as a numerical solution and the numerical model outcome is validated using the analytical solution. From this model validation, it is concluded that the model performs very good. The numerical experiments find the same final-state results compared to the analytical solutions. This means that we can use both the numerical as well as the analytical solutions to compare the results from the theoretical condensation experiment by Spengler et al. (2011) to the results found by Makarieva et al. (2013). Furthermore, it is important to mention that both the analytical and numerical approach are used to find the pressure perturbations in the cases with only latent heating, only mass removal and the two mechanisms combined.

## 2.3 Adjusting and comparing the experiments

The methods for quantifying the effect of condensation on surface pressure changes and latent heat release of both papers are different and yield different results. Due to the different experimental setup of the experiments, the results cannot be compared to each other 1:1. To be able to make a 1:1 comparison of the quantified effects of condensation on surface pressure and latent heating, the exact same amount of water vapor has to be condensed during the experiments. As the paper by Makarieva et al. (2013) is of main interest in this research, their modelling setup will be adjusted to match the one by Spengler et al. (2011). In subsection 2.3.1, an equation is derived to determine how much water vapor is being condensed in the condensation experiment by Makarieva et al. (2013). Subsection 2.3.2 describes the method by which the amount of condensate can be lowered in the condensation experiment by Makarieva et al. (2013).

### 2.3.1 Amount of condensate

As mentioned in the previous section, regarding the condensation experiment by Spengler et al. (2011), an exact amount of water vapor mass per unit area, $m_w = 0.2$ $kg/m^2$, is condensed. To achieve this with the condensation experiment by Makarieva et al. (2013), some adjustments and additions have to be made to the experimental setup of the original condensation experiment that was described in the paper by Makarieva et al. (2013) (section 2.1).

First of all, an equation is needed to quantify how much water vapor is being condensed in the condensation experiment by Makarieva et al. (2013). In the condensation experiment by Makarieva et al. (2013), the amount of condensate is equal to the total amount of water vapor present in the isothermal atmosphere (before applying the lapse rate) minus the total amount of water vapor present in the non-isothermal atmosphere (after applying the lapse rate). Therefore, equation 2.20 (that applies to the condensation experiment by Spengler et al. (2011)) has to be expanded to equation 2.23 for the condensation experiment by Makarieva et al. (2013).

$$m_w = \int_{z_1}^{z_2} \rho_{v,i}(z)dz - \int_{z_1}^{z_2} \rho_{v,ni}(z)dz \qquad (2.23)$$

Here, $\rho_{v,i}(z)$ is the density in the isothermal air column and $\rho_{v,ni}(z)$ is the density in the non-isothermal air column. The first integral in equation 2.23 thus represents the total mass of water vapor in the isothermal atmosphere, whereas the second integral represents the amount of water vapor in the atmosphere after applying an adiabatic lapse rate. In the isothermal atmosphere, the distribution of water vapor is solely determined by the hydrostatic balance and can thus be described by equation 2.11. By integrating equation 2.11 and using the ideal gas law of water vapor to find an expression for $\rho_v$, we end up with equation 2.24 for the density in an isothermal atmosphere.

$$\rho_{v,i}(z) = \rho_{v0} \exp\left(\frac{z}{h_n}\right) \qquad (2.24)$$

In the non-isothermal atmosphere, the distribution of water vapor is both determined by the hydrostatic balance and the Clausius-Clapeyron equation. The density in the non-isothermal atmosphere is therefore determined by equation 2.25.

$$\rho_{v,ni}(z) = \rho_v(T_s)\frac{h_{ns}}{h_n(z)}\exp\left\{-\int_0^z \frac{dz'}{h_v(z')}\right\} \qquad (2.25)$$

The right hand sides of equations 2.24 and 2.25 can now be substituted into equation 2.23 (not shown). Note that $h_v$ and $h_n$ are the scale heights derived in equation 2.4 and 2.11, respectively. After substituting we end up with an equation for $m_w$, that allows to calculate the amount of water vapor that is being condensed in the condensation experiment by Makarieva et al. (2013) using known constants and parameters.

### 2.3.2 Changing initial parameters

In the condensation experiment by Makarieva et al. (2013), there are only 3 parameters that can be changed. These are the initial values of the surface temperature ($T_0$), the surface pressure ($p_0$) and the partial pressure of water vapor at the surface ($p_{v0}$). As discussed in subsection 2.1.2, the value of the initial surface pressure only depends on the amount of molecules in the air columns and is therefore equal for all scenario's. The initial value of the partial pressure of water vapor at the surface is a function of the surface temperature and can be approximated with the Arden-Buck approximation (equation 2.6). This leaves the initial value of the surface temperature as the only independent parameter that can be changed in this condensation experiment. Changing the value of $T_0$ changes the profile of the moist adiabatic lapse rate (through solving the ODE's) and subsequently changes the temperature and pressure profile in the air column. From equations 2.23, 2.24 and 2.25, it can be observed that the mass of condensate in return depends on the aforementioned profiles through the scale heights. Therefore, we are able to find a value for the initial surface temperature for which the mass of the water vapor that condenses during the condensation experiment, $m_w$, is exactly 0.2 $kg/m^2$.

The used initial values for the surface temperature ($T_s$), surface pressure ($p_0$) and surface water vapor pressure ($p_{v,0}$) to solve the ODE's for which the mass of condensate is equal to 0.2 $kg/m^2$, can be found under set 4 in table 2.1. With these new values, we can recalculate what the pressure difference between the moist and dry column is, by again going through the steps described in section 2.1. The nonphysically low initial surface temperature of 214 K, needed to condensate 0.2 $kg/m^2$ of water vapor, is a result of the setup of the condensation experiment by Makarieva et al. (2013). By applying the moist adiabatic lapse rate to an (previously) isothermal air column results in large amounts of condensate for relatively low surface temperatures. This is due to the fact that the mass of condensate is determined by the difference of water vapor present in the isothermal and non-isothermal column over the entire column (equation 2.20) in combination with the exponential form of the Clausius-Clapeyron equation.

# 3 | Results

In this chapter, the results of the theoretical condensation experiments are presented. The chapter is divided in three sections. In **section 3.1** the results of the replica experiment are presented and discussed. In section **3.2**, the mass of condensate is calculated for the varying value of the initial surface temperatures being used in the condensation experiment by Makarieva et al. (2013). **Section 3.3** covers the outcome of the adjusted condensation experiment and compares it to the condensation experiment by Spengler et al. (2011). In **section 3.4**, the non-linear relation between the mass of condensate and the effect of latent heat release is explained using a proxy for the pressure gradient force.

## 3.1 Replica experiment Makarieva et al. (2013)

The results of the replica experiment are summarized in figures 3.1 and 3.2. As mentioned in section 2.1.2, the initial parameter values from table 2.1 have been used to solve the set of ODE's (eq 2.2, 2.4 and 2.5). By solving the set of ODE's, the pressure profiles for the three different surface temperatures are obtained. These pressure profiles have been plotted in subfigure 3.1a. The three pressure profiles have the same surface pressure, equal to the initial value of pressure, $p_0$, used to solve the ODE's. With increasing height, the pressure decreases for all three profiles, but with a different rate. The colder the temperature in the column, the faster the pressure decreases with height. This can be explained by the fact that the colder air contains molecules that have less energy compared to warmer air and therefore there are less collisions between molecules.

Subfigure 3.1b shows the moist adiabatic lapse rate for the used surface temperatures as well as the dry adiabatic lapse rate. It can be observed that the dry adiabatic lapse rate (black) is constant with height, whereas the moist adiabatic lapse rate ($\Gamma_m$) increases with height. Both the value of the moist adiabat at the surface and the rate at which the moist adiabat increases with height depend on the temperature of the atmospheric column. The moist adiabatic lapse rate becomes approximately equal to the dry adiabatic lapse rate at different heights. This is due to the decreasing amount of water vapor with temperature and therefore the reduced potential for latent heat release. The rate at which water vapor decreases with height is governed by both the Clausius-Clapeyron equation and hydrostatic equilibrium and is thus strongly dependent on the surface temperature and surface pressure.

By applying the moist and dry adiabatic lapse rates to the moist and dry isothermal atmospheric columns respectively, the temperature profiles in the non-isothermal columns are obtained. Subfigure 3.1c, shows the temperature profiles of the moist (solid) and dry (dashed) atmospheric column for the case in which the surface temperature is equal to 303 K. The fact that the moist adiabatic lapse rate takes on lower values compared to the dry adiabatic lapse rate has a clear effect on the temperature profiles. Close to the surface the moist and dry temperature profile are still comparable, but at a height of about 10 km the temperature difference becomes approximately 35 K.

The effect of latent heat release during condensation on temperature and pressure (related through the ideal gas law 1.2) is clearly visible from subfigures 3.1b and 3.1c. The moist column has higher values for temperature at any height compared to the dry column. However, the effect of condensation on the amount of molecules in the atmosphere and the subsequent hydrostatic adjustment are not yet incorporated in in these two figures. For that, we need subfigure 3.1d. The black line in this subfigure depicts the magnitude of the surface pressure perturbation, $\delta p_s$, for a range of surface temperatures in the (non)-isothermal atmospheric columns, calculated using equation 2.9. The colored dots represent the values of the surface pressure perturbation for the temperatures used in this replica study. The orange line in this subfigure shows the magnitude of the water vapor pressure, $p_v$, for the same range of surface temperatures. The water vapor pressure has been plotted for two reasons: (1) to show that the surface pressure perturbation follows a similar yet less strong exponential decay as the water vapor pressure for decreasing temperatures and (2) to point out that there is a mistake in figure 1b (page 1043) presented in the paper by Makarieva et al. (2013) (see figure A.1 in the appendix). The variable that has been plotted in that figure is the water vapor pressure instead of the surface pressure perturbation. This small mistake does not influence the outcome of the paper, since the other results use the surface pressure pertur-

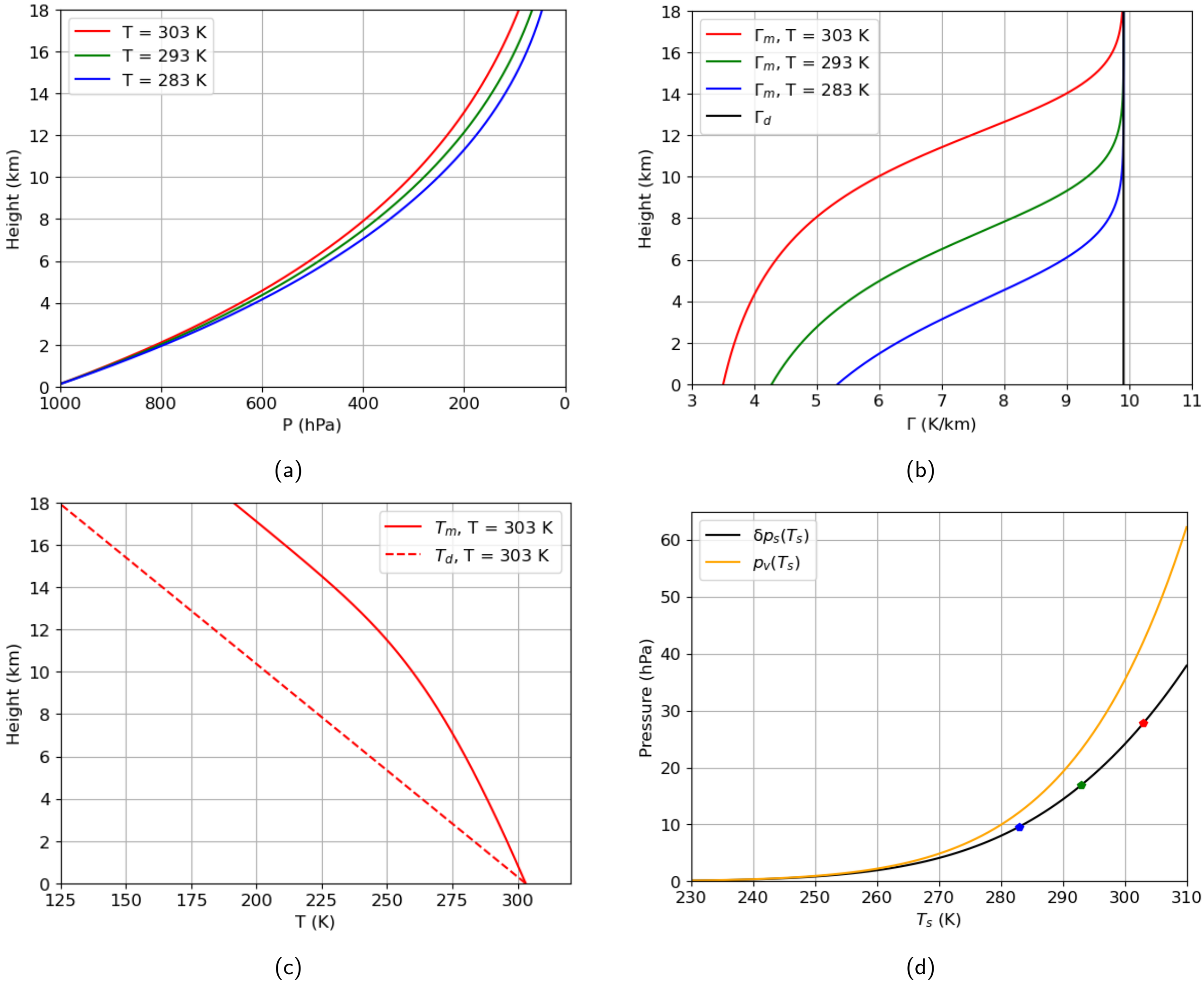


Figure 3.1: *These figures represent part of the results of the replica study. The initial parameters sets that are used to find these results can be found in table 2.1. In subfigure (b), the moist (color depending on temperature) and dry (black) adiabat are shown. The temperature profiles that result from applying the moist (solid) and dry (dashed) adiabat to the isothermal columns (for $T_s = 303$ K) are shown in subfigure (c). Subfigure (d) shows both the partial pressure of water vapor (orange) and the surface pressure perturbation (black) for a range of surface temperatures, $T_s$. The three colored dots in subfigure (d) represent the values of the surface pressure perturbation, $\delta p_s$, for the three surface temperatures being used in this replica study.*

bation instead of the water vapor pressure.

Both the effect of latent heat release and mass removal have now been quantified. By calculating the pressure profiles in both the moist and dry column using equations 2.13 and 2.14 and subsequently subtracting them from each other ($P_A - P_B$), we end up with subfigure 3.2a. The original figure showing the pressure difference between column A and column B that is presented in the paper by Makarieva et al. (2013), is shown in subfigure 3.2b. Mass removal lowers the atmospheric pressure at the surface, whereas latent heat release increases the atmospheric pressure throughout the column. Therefore, the negative value in surface pressure difference between the two columns in subfigures 3.2a and 3.2b represents the effect of mass removal, whereas the effect of latent heat release can be observed from the increasing pressure difference with height. Based on the subfigures in figure 3.2, we can draw the following conclusions:

Firstly, subfigure 3.2a is identical to subfigure 3.2b, except for the height range over which the pressure difference is plotted. This means that the replica condensation experiment was correctly executed.

Secondly, the values of the surface pressure perturbation for the temperature used in this replica study (colored dots subfigure 3.1d) are equal to the pressure difference at the surface for the different temperatures (subfigure 3.2a and 3.2b). If we for example focus on the red line ($T_s = 303K$), then we see that at the surface, the pres-

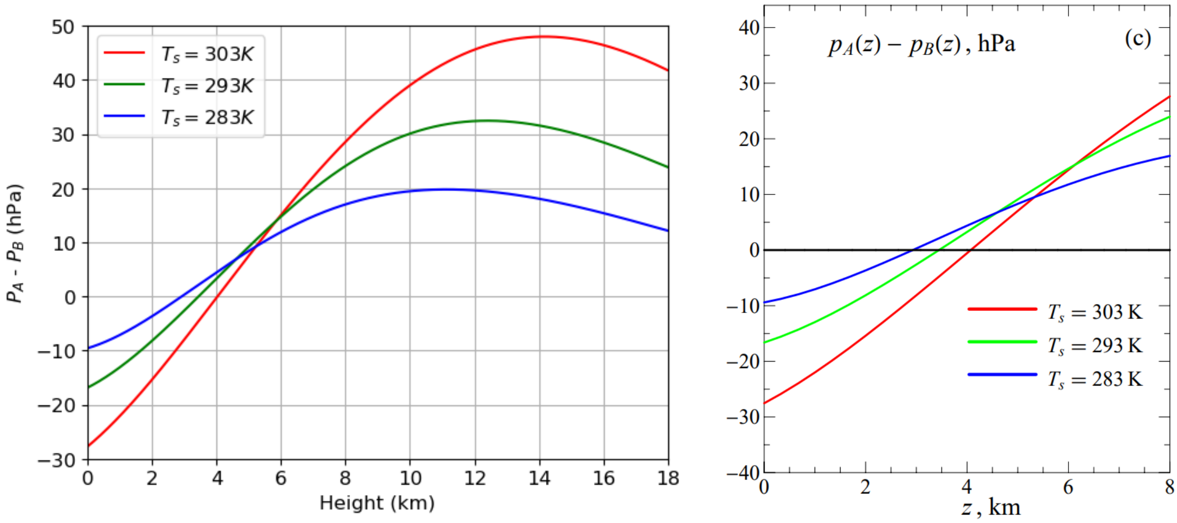


(a) (b)

Figure 3.2: *The pressure difference between column A and column B over the height of the columns for the three surface temperatures. Figure (a) shows the result of the replica study, whereas figure (b) is taken from Makarieva et al. (2013) and shows the result of the original experiment.*

sure difference between column A (moist) and B (dry) is about -28 hPa instead of -42 hPa. Therefore, we can conclude that, although their figure 1b (see appendix figure A.1) incorrectly plots the water vapor pressure, the authors did correctly use the surface pressure perturbation instead of the water vapor pressure in the calculations for the pressure profile of column A.

Thirdly, if we again focus on the red line ($T_s = 303K$) in the lower 8 km of the atmosphere in subfigure 3.2a and subfigure 3.2b, it can indeed be observed that there is no clear latent heating dominance. At a height of about 4 km, the pressure difference between the columns is 0 hPa. Below that height the reduction in surface pressure due to the mass removal following condensation dominates, whereas the effect of latent heating dominates above a height of 4 km. However, above 8 km height, the pressure difference between column A and B is still increasing hinting at a stronger (not yet dominant) effect of latent heating. There is no explanation in the paper by Makarieva et al. (2013) why only the lower 8 km of the atmospheric columns are taken into account.

Lastly, all three lines plotted in figure 3.2a, representing a certain initial surface temperature, show that the pressure difference between column A and B decreases above a certain height. This height ranges from about 10 km (blue line) to 14 km (red line). Pressure in the atmospheric columns decreases with height and will inevitably reach 0 Pa at a given height (see figure 3.1a). The decrease in pressure difference between the moist and dry column above a certain height, as observed in figure 3.2a, is a result of the decreasing pressure with height in columns A and B and not a remnant of the effects of either mass removal or latent heat release. That is, if the pressure in both the moist and dry atmospheric column approach 0 Pa, the pressure difference between the two columns will tend to decrease as well with height. This effect and it's implications for this research will be further discussed in section 3.4.

## 3.2 Mass of condensate

The figures of the replica study, suggest that there is no latent heat dominance for the initial surface temperatures used in this study. However, it is not clear from the paper by Makarieva et al. (2013) how much water vapor is being condensed. Therefore, the method described in section 2.3 is used to calculate the amount of water vapor that is being condensed during the condensation experiment by Makarieva et al. (2013). For this calculation, the density profiles of water vapor in the (non-)isothermal atmosphere are needed. These can be calculated using equation 2.24 and 2.25. The density profiles for the isothermal and non-isothermal atmospheres are shown in figure 3.3 for the three different surface temperatures being used in the original and replica study. With equation 2.23, the mass of water vapor condensate can be calculated. The mass of water vapor condensate, $m_w$, is equal to the shaded areas in figure 3.3 for the three different temperatures if the equation is integrated from $z = 0$ to $z \to \infty$.

Figure 3.3 shows that the amount of water vapor that is

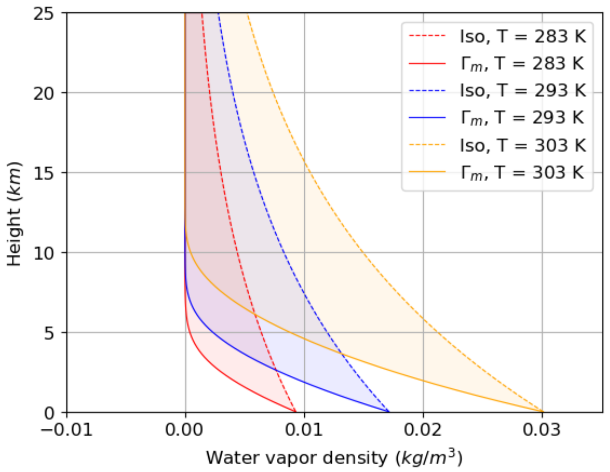


Figure 3.3: *The density profiles for the three surface temperatures being used in the original and replica experiment for the isothermal and non-isothermal atmosphere. The shaded areas represent the amount of water vapor that is being condensed when the moist adiabatic lapse rate is applied.*

being condensed due to applying a moist adiabatic lapse rate to an isothermal atmosphere, strongly depends on temperature. There is a clear non-linear relationship between the surface temperature being used in the condensation experiment and the mass of condensate. The exact values of the mass of water vapor that is being condensed as a result of applying the moist adiabatic lapse rate are provided in table 3.1, but will be further discussed in section 3.3.

## 3.3 Experiment comparison

To compare the two condensation experiments by Makarieva et al. (2013) and Spengler et al. (2011), the amount of water vapor that condenses over the entire atmospheric column, $m_w$, in the experiments has to be equal. Therefore, the amount of condensate in the experiment by Makarieva et al. (2013) has been adjusted according to the methods described in section 2.3. The values of the surface temperature, pressure and water vapor partial pressure for which $m_w$ = 0.2 $kg/m^2$ can be found in table 2.1 under set 4. These values have been used to recalculate the pressure difference between the moist and dry column by going through the steps described in section 2.1.

The results of the adjusted experiment by Makarieva et al. (2013) (left) and the condensation experiment conducted by Spengler et al. (2011) (right) are presented in figure 3.4. Due to the experiment setup by Spengler et al. (2011) (as described in section 2.2), the pressure difference in the column is provided for $t = 0$ (dashed line) and $t \to \infty$ (solid blue line). The dashed line represents the pressure difference in the column at the moment when all water vapor is being condensed, whereas the solid line represents the pressure difference after hydrostatic adjustment occurred and the system is back in hydrostatic equilibrium. As mentioned in section 2.2, water vapor is only present in the layer between 4 and 6 km height. A strong latent heating effect can be observed in this layer at $t = 0$, as there is a pressure increase of about 0.8 hPa throughout this layer. In addition, there is a small pressure decrease below the layer where the water vapor is being condensed. This pressure decrease at $t = 0$ is not due to the mass removal effect, but due to the setup of the experiment in which a initial pressure perturbation was calculated due to the fact that water vapor is lighter than dry air (see section 2.2). The difference between the surface pressure perturbation resulting from water vapor being lighter than dry air and the surface pressure perturbation resulting from the mass removal effect is illustrated in figure 3.5. In figure 3.5, there is a surface pressure perturbation present at $t = 0s$ of about -0.023 hPa, which is related to the fact that water vapor is lighter than dry air. The surface pressure than evolves over time until the equilibrium state is reached at $t = 500s$. In this equilibrium state the surface pressure perturbation is equal to about -0.043 hPa, which is the result of the mass removal effect and the initial pressure perturbation combined. Therefore the mass removal mechanism itself results in a pressure perturbation of about -0.02 hPa.

For the experiment comparison, we mainly focus on the solid blue line in figure 3.4 representing the equilibrium state, because it can be compared to the outcome of the experiment by Makarieva et al. (2013).

The two subfigures presented in figure 3.4 show quite some resemblance:

- There is a small pressure perturbation at the surface as a result of the mass removal due to condensation.
- Pressure increases through latent heat release in the layers of condensation.
- The effect of latent heating is dominant over the effect of mass removal.
- The maximum pressure difference is reached at ap-

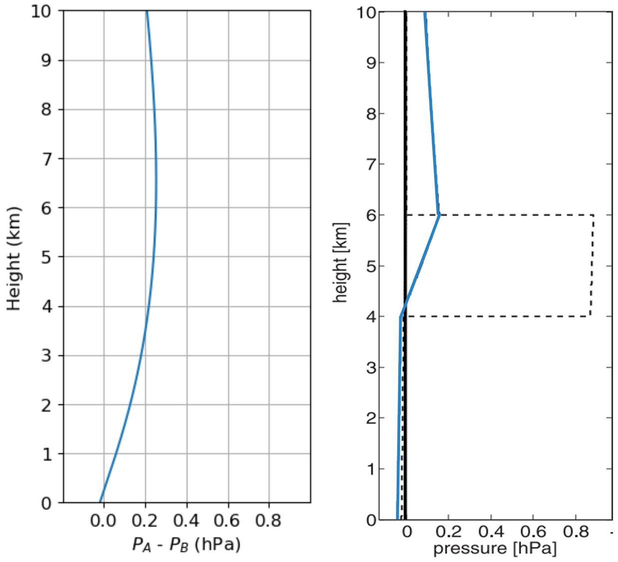


Figure 3.4: *The comparison between the result of the adjusted condensation experiment by Makarieva et al. (2013) (left) and the experiment by Spengler et al. (2011) (right). The left figure shows the pressure difference between the moist (A) and dry (B) column over height. The right figure shows the result of the analytic solution experiment with latent heating and mass removal, with $p = 0$ (solid black line), $t = 0$ (dashed line) and $t \to \infty$ (solid blue line). Note that the right figure is adapted from Spengler et al. (2011).*

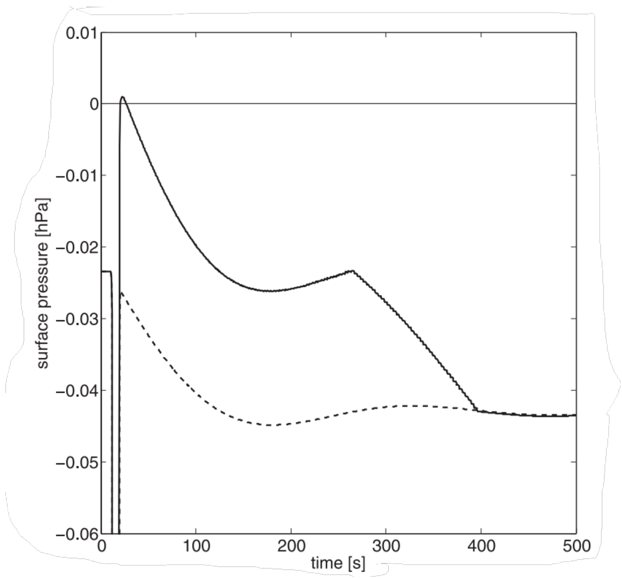


Figure 3.5: *The surface pressure perturbation over time as found in the numerical solution of the theoretical condensation experiment by Spengler et al. (2011), by only including mass removal. The solid line gives the surface pressure perturbation for the simulation with falling rain, whereas the dashed line gives the surface pressure perturbation for the simulation without falling rain. This figure is taken form Spengler et al. (2011).*

proximately 6 km's height.

- Above the maximum pressure difference height, the pressure difference starts to slowly decrease again.

There are however also some differences that need mentioning, such as the magnitude of the surface pressure perturbation, $\delta p_s$. This perturbation is equal to 1.95 Pa for the adjusted experiment by Makarieva et al. (2013), but about 4.2 Pa in the experiment by Spengler et al. (2011). However as explained before, the surface pressure perturbation that results from the mass removal mechanism in the experiment by Spengler et al. (2011) is equal to about 2 Pa. Therefore, the surface pressure perturbation that result from mass removal in the theoretical condensation experiments by Spengler et al. (2011) and Makarieva et al. (2013) are approximately equal. Another difference between the two experiments is the layer in which the condensation takes place. The experiment by Spengler et al. (2011) only condenses water in the layer between 4 and 6 km. That results in the fact that the experiment by Spengler et al. (2011) shows that the pressure starts to increase from 4 km onward, because the latent heating only affects the pressure within and above the layer that is heated. This was also observed by the study on which the experiment by Spengler et al. (2011) was build (Bannon, 1995). Due to the setup of the experiment by Makarieva et al. (2013), water vapor condenses over the entire height of the atmospheric column. This can also be observed in the pressure difference profile in figure 3.4, where the pressure difference first becomes less negative and afterwards positive just above the surface. Furthermore, the maximum pressure difference is about 25 and 18 Pa for the condensation experiment by Makarieva et al. (2013) and Spengler et al. (2011), respectively. Based on the fact that pressure starts to increase from the surface onward in the condensation experiment by Makarieva et al. (2013) and reaches a higher maximum value compared to the condensation experiment by Spengler et al. (2011), it seems that the latent heating dominance is stronger in the condensation experiment by Makarieva et al. (2013). This will be further discussed in section 4.2.

Now that the condensation experiments of both papers are set up in such a way that there is 0.2 $kg/m^2$ of water vapor being condensed, the contradiction in their results seem to fade away. Both show that for this setup there is a clear latent heating dominance. In table 3.1, the most important results of the experiments are summarized. For the 4 initial surface temperatures being used in this, as well as for the average atmospheric temperature being used in the study by Spengler et al. (2011), the values for the amount of condensed water vapor ($m_w$), the maximum pressure difference due to latent heating (max.), the surface pressure perturbation ($\delta p_s$) and the ratio between the maximum pressure difference and the surface pressure perturbation ($\frac{max.}{\delta p_s}$) are provided. Table 3.1 shows that the ratio between the surface pressure perturbation and the maximum value of the pressure difference is larger for the adjusted experiment by Makarieva et al. (2013) (about 13.3) than for the experiment by Spengler et al. (2011) (about 9). This result indicates an even stronger latent heating dominance for the experiment by Makarieva et al. (2013) compared to the experiment by Spengler et al. (2011).

Furthermore, from table 3.1 some interesting relations between variables can be deduced. The exponential relation between mass of condensate and temperature, which is also shown in figure 3.3, is due to the exponential relation between air temperature and saturation vapor pressure (Clausius-Clapeyron, see equation 2.1). In addition, there is a linear relation between the surface pressure perturbation and the mass of condensate: if the amount of condensate is doubled, the resulting pressure difference at the surface is doubled as well. As a result of the previous two relations, there must be an exponential relation between the surface pressure perturbation and temperature, which can be observed in the table and is also shown in subfigure 3.1d.

Interestingly for this research however, is the fact that the maximum value for the pressure difference as a result of latent heat release does not show a linear relationship with the amount of condensate. For low values of $m_w$, the maximum pressure difference remains quite high compared to the values of the surface pressure perturbation. Interpreting this result is not so straightforward. When water vapor condenses a certain amount of latent heat is released, which is a molecular property. When the amount of water vapor being condensed is doubled, it is expected that the amount of latent heat being released is doubled too. An explantion of these results is provided in the following section (section 3.4).

## 3.4 Pressure gradient force

In the previous section, it is shown that there is a linear relation between the mass of condensate ($m_w$) and surface pressure perturbation ($\delta p_s$), but a non-linear relation between the mass of condensate and the maximum pressure difference between the moist and dry atmospheric columns. However, it is expected that both of these relations are approximately linear: doubling the mass of condensate leads to a doubling in the surface pressure perturbation (due to mass removal) and a doubling in the maximum pressure difference (due to latent heat release).

In the last paragraph of section 3.1, an explanation is provided for the decrease in pressure difference between the moist and dry column above a certain height (see figure 3.2a). It is argued that this decrease in pressure difference above a certain height is not an effect of the latent heat or mass removal mechanism, but due to the pressure decrease with height in both the moist and dry column. In the condensation experiment by Makarieva et al. (2013), the effect of mass removal on atmospheric pressure is bound to the surface and the lower atmosphere, but the effect of latent heat release occurs through the entire atmospheric column. Therefore, it is likely that the magnitude of the pressure difference that results from latent heating (higher up in the air colum) is affected by the decreasing pressure in both columns. The pressure gradient force (equation 3.1) can be used to show the pressure difference between the moist and dry column when the effect of decreasing pressure with height is included. As the condensation experiment by Makarieva et al. (2013) is theoretical, there is no distance defined between the moist an dry column. Therefore, the pressure difference divided by the density will be used, which can be seen as a proxy for the pressure gradient force.

$$F_{p,x} = -\frac{1}{\rho}\frac{\partial p}{\partial x} \tag{3.1}$$

Table 3.1: *Values for the surface pressure perturbation (due to mass removal), the maximum pressure difference (due to latent heating) and their ratio are provided as well as the mass of water vapor being condensed. The values are given for the three surface temperatures being used in the original condensation experiment by Makarieva et al. (2013) and the surface temperature being used in the adjusted experiment. In addition, the values are given for the experiment by Spengler et al. (2011).*

| | $T_s$ (K) | $T_{avg}$ (K) | $m_w$ $(kg/m^2)$ | max. (Pa) | $\delta p_s$ (Pa) | $\frac{max.}{\delta p_s}$ (-) |
|---|---|---|---|---|---|---|
| Mak | 214 | Na | 0.2 | 25 | 2 | 13.3 |
| | 283 | Na | 105.3 | 1975 | 961 | 2.1 |
| | 293 | Na | 190.7 | 3245 | 1692 | 1.9 |
| | 303 | Na | 319.6 | 4798 | 2781 | 1.7 |
| Spe | Na | 255 | 0.2 | 18 | 2 | 9 |

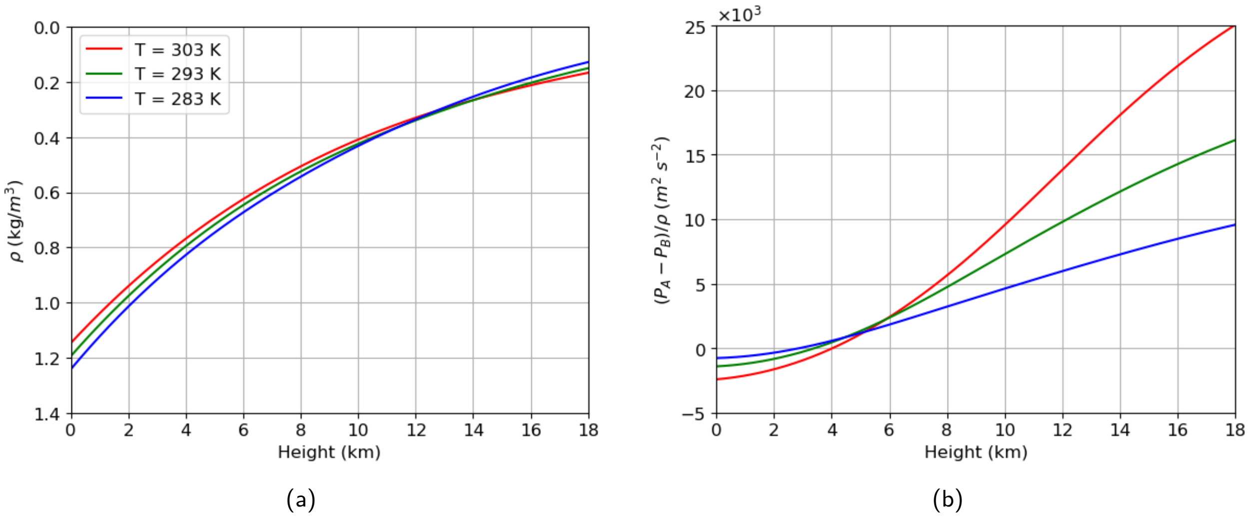


Figure 3.6: *Subfigure (a) shows the density profiles for the three different surface temperatures used in the condensation experiment by Makarieva et al. (2013). Subfigure (b) shows the pressure difference (subfigure 3.2a) divided by the density, which is used in this research as a proxy for the pressure gradient force.*

Here $F_{p,x}$ is the pressure gradient force in the horizontal direction, $\rho$ is the density and $\frac{\partial p}{\partial x}$ is the pressure difference over a horizontal distance. It is the pressure gradient force and not the pressure difference that moves fluids around in the ocean and atmosphere.

Subfigure 3.6a shows the density profiles for the three initial surface temperatures being used in the original condensation experiment by Makarieva et al. (2013). Subfigure 3.6b shows the pressure difference between the moist and dry columns (see subfigure 3.2a) divided by the density for the three initial surface temperatures. Both graphs are also made for the initial surface temperature of 214 K (see appendix figure A.2), but excluded from figure 3.6 because the values are two orders of magnitude smaller. From figure 3.6b, it can be concluded that the proxy for the pressure gradient force depends on temperature. Similar as in figure 3.2a, the negative values of the proxy for the pressure gradient force represent the effect of mass removal. The lowest value is found at the surface, above which the latent heating effect will act to increase the proxy for the pressure gradient force. The heights at which the mechanisms balance is the same as in 3.2a. Subfigure 3.6b clearly shows that the effect of latent heating is dominant, because the proxy for the pressure gradient force reaches values that are more than an order of magnitude larger than the values at the surface. This result differs a lot from the original figure showing only the pressure difference as presented in the paper by Makarieva et al. (2013) (see figure 3.2b). Nevertheless, figure 3.6b shows that the mass removal effect is not negligible in the lower atmosphere for the used initial surface temperatures. However, the magnitude of the negative values that are due to the mass removal effect and the height at which the two mechanisms balance quickly decrease with decreasing initial surface temperature and thus decreasing mass of condensate. Both condensation experiments show that for small amounts of condensate, the effect of mass removal and the height at which the two mechanisms balance are negligible (see figure 3.4 and A.2).

These findings explain why the papers by Makarieva et al. (2013) and Spengler et al. (2011) ended up with such different conclusions: one claiming that there is a latent heating dominance, whereas the other claims that the effect of mass removal is underestimated. Even though the two condensation experiments were set up in a different way, the results are not that different when the same amount of water vapor is being condensed. However, the results (and therefore the conclusions) will change when more mass of water vapor is being condensed if the pressure difference is expressed as in the paper by Makarieva et al. (2013). The proxy for the pressure gradient force shows a latent heating dominance for all used initial surface temperature values.

# 4 | Discussion

In this research, two theoretical condensation experiments used to quantify the effect of latent heat release and mass removal on atmospheric pressure are investigated and compared to each other. In **section 4.1** and **4.2** the results of this comparison are discussed focusing on the mass removal and latent heat release mechanisms respectively. The results of this research points out that the effect of mass removal in the lower atmosphere should be taken into account for relatively large amounts of condensate. In **Section 4.3**, the time scale associated with the mass removal effect of these large amounts of condensate is estimated. The last section, **Section 4.4**, discusses the limitations of this research.
To put this research into context, some peer reviews of the paper by Makarieva et al. (2013) are used (Makarieva et al., 2011) throughout this chapter. To clarify which of the reviews are used, they are referred to with the same numbers that are being used on the website.

## 4.1 Mass removal

The comparison of the condensation experiments by Spengler et al. (2011) and Makarieva et al. (2013) shows that the effect of mass removal is approximately similar (about 2 Pa) when the same amount of water vapor is being condensed (see section 3.3). Arguably, as both methods yield similar results, it can be expected that atmospheric numerical models correctly include the effect of mass removal on atmospheric pressure when the magnitude of the mass removal in these models is in agreement with the findings such as the one by Spengler et al. (2011). An interesting discussion on the inclusion of the mass removal effect in an atmospheric numerical model by Anastassia Makarieva (main author of the paper Makarieva et al. (2013)) and George Bryan (developer of the model of interest) can be found in the following reviews: AC C10926, SC C11194 and AC C12008.
Furthermore, it is important to note that not only the magnitude of the mass removal effect on atmospheric pressure decreases with decreasing mass of condensate, but also the height at which the effect of mass removal dominates over the effect of latent heat release (resulting in negative pressure differences in the lower atmosphere). This is clearly observed in subfigure 3.2a, where this height decreases from 4 km to about 2.5 km for the different temperatures (and thus masses of condensate) being used. The left figure in figure 3.4 shows that this height has decreased to about 200 metres for 0.2 $kg/m^2$ of condensate. These findings suggest that low amounts of precipitation do not contribute to the circulation as proposed in the paper by Makarieva and Gorshkov (2007) (see section 1.2 and 1.3), because both the magnitude of the mass removal effect as well as the height at which the pressure decreases due to condensation is negligible.

## 4.2 Latent heat release

In the review 'AC C14894', written by the main author of the paper, it is said that: "*the statement that latent heat release is more important for atmospheric dynamics than the vapor sink could only be substantiated by considering a physically plausible process*". This quote refers to the claim that the theoretical condensation experiment by Spengler et al. (2011) is incorrect and that the condensation experiment by Makarieva et al. (2013) is physically correct. According to the author, the condensation experiment by Spengler et al. (2011) is incorrect due to the fact that it is assumed that adiabatic condensation occurs spontaneously at constant volume. In this review the author refers to section 2 and 3 of the paper by Makarieva et al. (2013), to show that adiabatic condensation cannot occur at constant volume. In this research, we do not claim to know which one of the experiments is wrong or correct. However, using the theoretical condensation experiment by Makarieva et al. (2013), we have shown that the two condensation experiments yield similar results if the same mass of water vapor is being condensed.
What is striking, is that the experiment comparison shows that the effect of latent heating is stronger in the adjusted condensation experiment by Makarieva et al. (2013) (see section 3.3). This could possibly be caused by the claim made in the quote mentioned above, that adiabatic condensation is calculated at constant volume. Yet, this strongly contradicts one of the main conclusions in the paper by Makarieva et al. (2013), that the effect and magnitude of mass removal are overlooked and wrongly assumed to be small. If the reasoning and methods in the paper by Makarieva et al. (2013) are

followed, but adjusted in such a way that we can correctly compare it to the study by Spengler et al. (2011), it can be concluded that the effect of mass removal in both condensation experiments is approximately equal, but that the latent heating dominance is even more pronounced than pointed out by Spengler et al. (2011).

## 4.3 Time scales

In previous sections it is shown that, even though there is a latent heating dominance, the effect of mass removal can dominate in the lower atmosphere when considering large amounts of condensate. However, the time scale that is associated with such large amounts of condensate is an important aspect when considering the mass removal mechanism as a driver of atmospheric dynamics.

The surface temperatures used in the original condensation experiment by Makarieva et al. (2013) yield large amounts of condensate. The mass of water vapor being condensed in the atmospheric column for $T_s = 303$ K is 320 $kg/m^2$. Note that 1 $kg/m^2$ is approximately equal to 1 mm of precipitation.

If the removal of water vapor molecules from the atmosphere results in a decrease in air pressure in the lower atmosphere, then the addition of water vapor molecules to the atmosphere through evaporation must have the opposite effect. This is acknowledged in the paper by Makarieva et al. (2013), but the authors explain that the effect of condensation dominates over the effect of evaporation. Nevertheless, the moisture convergence (precipitation minus evaporation) should be used, when estimating the time scales associated with the amount of water vapor being condensed in the original and replica experiment by Makarieva et al. (2013). Moreover, in order for the biotic pump circulation to work (see section 1.2 and 1.3), the netto effect of precipitation and evaporation on atmospheric pressure has to be larger over continents than over the oceans. Here, the moisture convergence over the Amazon region and the adjacent ocean region are compared to derive the time scales that are associated with the effect of mass removal on atmospheric pressure. Even though there are two ocean regions that surround the Amazon Basin (the Eastern Pacific and the Atlantic Ocean), the tropical Atlantic region acts as the most important remote source of moisture for the Amazon Basin (Drumond et al., 2014). Therefore, the moisture convergence over the Amazon region will be compared to the moisture convergence over the Atlantic Ocean.

Marengo (2006) estimated that the yearly precipitation in the Amazon Basin is about 2215 mm/year with a standard deviation of about 180 mm/year. In addition, according to da Motta Paca et al. (2020), the average daily evaporation in the Amazon Basin is 2.83 mm/day (corresponding to about 1033 mm/year). The moisture convergence thus equals: $P - E = 2215 - 1033 = 1182$ mm/year. Estimates for the moisture convergence or divergence over the Atlantic Ocean, are derived from a study by Brown and Kummerow (2014). They estimated the moisture convergence for five tropical (between 15°S–15°N) ocean regions for the period between 1998 and 2007. The five tropical ocean regions are: the Indian Ocean (TI), the Western Pacific (TWP), the Central Pacific (TCP), the Eastern Pacific (TEP) and the Atlantic region (TA). The values that are provided are retrieved from reanalysis data. Figure 4.1 shows the divergence ($\nabla Q$), which is equal to the freshwater flux ($E - P$) when averaged over longer times, for two reanalysis data sets (ERA and MERRA).

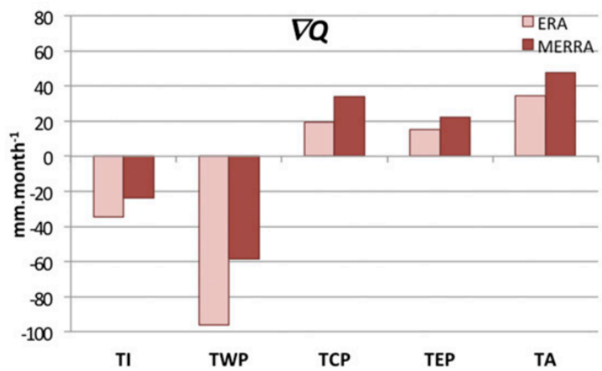


Figure 4.1: *Divergence ($\nabla Q$) over 5 tropical ocean regions: the Indian Ocean (TI), the Western Pacific (TWP), the Central Pacific (TCP), the Eastern Pacific (TEP) and the Atlantic region (TA). Data is from two reanalysis data sets (ERA and MERRA) sets over the period 1998 to 2007. This figure is adopted from Brown and Kummerow (2014).*

Figure 4.1 indicates that there is moisture convergence over the Indian Ocean and the Western Pacific, but moisture divergence over the Central Pacific, Eastern Pacific and Atlantic Ocean. Based on this reanalysis data, the moisture divergence over the tropical Atlantic Ocean region is about 35 mm/month (ERA) or 45 mm/month (MERRA), corresponding to about 420 mm/year and 540 mm/month respectively. Therefore, the netto estimated difference of moisture convergence/divergence over the Amazon Basin and the tropical Atlantic ocean region adds up to about 1600 - 1720 mm/year. This means that the surface pressure perturbation of 28 hPa, corresponding to the surface temperature of 303 K in the experiment by Makarieva et al. (2013), could be achieved in a little more than 2 months. This is equal to about 0.5 hPa per day.

Estimating the time scales shows that the effect of condensation on atmospheric pressure, as presented in the paper by Makarieva et al. (2013), is not instantaneously achieved. The pressure differences that occur due to the large amounts of condensate are spread out over a prolonged time period. Combined with the latent heating dominance as demonstrated in this research, it seems unlikely that the mass removal mechanism is the main driver of atmospheric dynamic instead of differential heating, because the effects sum up to a few pascals of pressure change per day. Certainly when considering that this is a relatively extreme example, because the Amazon region is one of the wettest regions of the planet. Figure 4.1 shows that the Atlantic Ocean has the strongest divergence. Therefore, it can be expected that the mass removal effect accounts for smaller pressure perturbation in the lower atmosphere in most other regions.

Even though these estimates are prone to uncertainties and differ a lot per region, they provide some insights in the time scales associated with the netto mass of condensate that affects the atmospheric pressure.

## 4.4 Limitations

There are two important limitations to this research that will be discussed here. The first one is associated with the comparison between the studies conducted by Makarieva et al. (2013) and Spengler et al. (2011). Due to time constraint, it was not possible during this research to adjust the condensation experiment by Spengler et al. (2011). This means that the condensation experiments can only be compared for the case where 0.2 $kg/m^2$ of water vapor is condensed. Therefore, it is not certain if the results of the comparison studies are consistent when different amounts of water vapor are condensed. However, it is expected that the condensation experiment by Makarieva et al. (2013) will consistently yield a stronger latent heating dominance compared to the condensation experiment by Spengler et al. (2011). That is because the relation between the mass of condensate and the amount of latent heat release, as well as the effect of mass removal, are expected to be linear.

Furthermore, this research focused mainly on the theoretical condensation experiments conducted by Makarieva et al. (2013) and Spengler et al. (2011). The theoretical condensation experiment that is presented in the paper by Makarieva et al. (2013) is however only a small share of all the theory presented in that paper and an even smaller share of all the theory presented in the papers on the condensation-induced atmospheric dynamics and biotic pump theory. Moreover, the author made the following statement on the theoretical condensation experiment in the review 'AC C14894': "*The results of Section 3 show that considering a physically plausible process (condensation by diabatic cooling) and involving relevant atmospheric parameters (moist versus dry adiabatic lapse rates) one obtains results incompatible with the statement about latent heat dominance. At the same time, these considerations do not prove that the calculated pressure differences can actually exist in the atmosphere. This is because the laws of equilibrium thermodynamics do not suffice to predict atmospheric dynamics. This is a more general argument against the latent heat dominance meme: a proposition that is based on (incorrect) thermodynamic considerations of condensation may have little implications for condensation-induced dynamics. This dynamics is considered in Section 4 of M10.*". In this statement, 'Section 3' refers to the section in Makarieva et al. (2013), where the theoretical condensation experiment is presented. 'Section 4 of M10' refers to a section in Makarieva et al. (2013) where an equation is presented to quantify the horizontal pressure gradients that result from condensation.

In this research we have shown that, using the methods of the theoretical condensation experiment by Makarieva et al. (2013), the latent heat release mechanism dominates over the mass removal mechanism. Therefore, the statement that the results presented in the paper Makarieva et al. (2013) are 'incompatible with the statement about latent heat dominance' is incorrect. Moreover, the author of the paper Makarieva et al. (2013) states in this comment that the results of the theoretical condensation experiment cannot be used to predict the atmospheric dynamics. According to the authors, the equations provided in 'Section 4 of M10' are needed to predict the atmospheric dynamics. Be that as it may, the equations for the horizontal pressure gradient derived in that section received a lot of criticism. We will not go into depth about the arguments presented in these reviews, but they are provided on the website where the discussion took place (Makarieva et al., 2011) in a set of reviews by Anastassia Makarieva (the author of Makarieva et al. (2013)) and Nick Stokes: 'SC C9174', 'AC C11046', 'AC C10922', 'SC C11071' and 'AC C12836'.

Nevertheless, to convince the scientific community that the mass removal effect associated with condensation is a main driver of atmospheric dynamics, we argue that the theoretical condensation experiment presented in the paper by Makarieva et al. (2013) does not suffice as a foundation for the claim that it is condensation that drives atmospheric dynamics instead of differential heating.

# 5 | Conclusion

This research aimed to contribute to either validating or disproving the biotic pump theory, as described by Makarieva and Gorshkov (2007), by investigating the condensation-induced dynamics as proposed in the paper by Makarieva et al. (2013). The authors of these papers claim that condensation is an important driver of large scale atmospheric dynamics and even argue that condensation might be more important than differential heating in the atmospheric circulation. In the paper by Makarieva et al. (2013), the methods and results for a theoretical condensation experiment are presented to substantiate these claims. Using this condensation experiment it is shown that condensation affects hydrostatic pressure in the atmosphere through two different mechanisms: latent heating and mass removal. These two mechanisms affect atmospheric pressure in opposite ways. Mass removal decreases atmospheric pressure underneath and within the layer of condensation, whereas latent heat release increases pressure within and above the layer of condensation. The results of the condensation experiment by Makarieva et al. (2013) suggest that the effect of mass removal is comparable in magnitude compared to the effect of latent heating (figure 3.2), but that the effects are spatially separated in the atmospheric air column: mass removal in the lower atmosphere and latent heating higher up in the atmosphere. These results contradict the established belief that the effect of latent heating dominates over the effect of mass removal. This latent heating dominance was pointed out in a paper by Spengler et al. (2011), who quantified the effect of mass removal and latent heating using a different theoretical condensation experiment.

In this research, the condensation experiment by Makarieva et al. (2013) is first replicated and subsequently adjusted in such a way that the amount of condensate is equal in both experiments. This is done by lowering the initial surface temperature, which determines the amount of condensate, until exactly 0.2 $kg/m^2$ of water vapor is being condensed. When the same amount of water vapor is being condensed, both theoretical condensation experiment point out that the effect of latent heat release dominates over the effect of mass removal (figure 3.4). In fact, the latent heating dominance is more pronounced in the condensation experiment by Makarieva et al. (2013). From this we can conclude that the divergent conclusions, based on the two condensation experiments, in the papers by Makarieva et al. (2013) and Spengler et al. (2011) are not necessarily a result of incorrect physical laws or assumptions, but can be retraced to the amount of water vapor being condensed in the experiments. To understand why different amounts of condensate yield different conclusion (regarding the latent heating dominance) for the experiment by Makarieva et al. (2013), a proxy for the pressure gradient force is used (figure 3.6). It shows that latent heating dominance also holds for larger amounts of condensate by taking into account that pressure and density are height dependent.

The results of this research thus show that, no matter which one of the two theoretical condensation experiments by Makarieva et al. (2013) and Spengler et al. (2011) is used, there is a clear latent heating dominance associated with condensation. Nevertheless, condensation can result in a significantly lowered atmospheric pressure in the lower atmosphere when large amounts of water vapor are condensed. Yet, these vast amounts of water vapor cannot condense instantaneously and therefore the time scales at which these pressure differences occur have to be taken into account. Using rough estimates, it is argued that the mass removal effect could potentially lead to a negative pressure difference of about 0.5 hPa for extreme cases. By both showing that latent heating is dominant and that the mass removal effects only amount up to a few Pa per day in extreme cases, it seems unlikely that it is the mass removal mechanism that drives atmospheric dynamics instead of differential heating.

The condensation-induced atmospheric dynamics and especially the mass removal effect is an essential part of the biotic pump theory. In this research the theoretical condensation experiments by Makarieva et al. (2013) and Spengler et al. (2011) are used as a basis to contribute to either validating or disproving the biotic pump theory. Even though the conclusion based on this research is that it is unlikely that mass removal drives atmospheric dynamics instead of differential heating, it is acknowledged that these experiments come with limitations. Essential to the biotic pump theory are the horizontal pressure gradients that arise due to condensation as explained in section 4 in the paper by Makarieva et al. (2013). As mentioned in the discussion of this research, this section received a lot of criticism. However, to be able to verify the validity of the biotic pump theory, the scientific community first has to agree on the validity of the theory presented in that section. Further research could also focus on the example of the cold Amazon paradox, which is mentioned in section 1.4. Looking into the capability of climate models to simulate events such as the cold Amazon paradox, could clarify if this paradox is a result of a missing feedback mechanism in the model (such as the biotic pump) or a result of other mechanisms (other possible mechanisms are mentioned in the paper by Sheil (2018)) that are included in climate models.

# Bibliography


Bannon, P.R., 1995. Hydrostatic adjustment: Lamb's problem. Journal of the atmospheric sciences 52, 1743–1752.

Bannon, P.R., Chagnon, J.M., James, R.P., 2006. Mass conservation and the anelastic approximation. Monthly weather review 134, 2989–3005.

Baudena, M., Tuinenburg, O.A., Ferdinand, P.A., Staal, A., 2021. Effects of land-use change in the amazon on precipitation are likely underestimated. Global Change Biology 27, 5580–5587.

Bonan, G.B., 2008. Forests and climate change: forcings, feedbacks, and the climate benefits of forests. science 320, 1444–1449.

Brown, P.J., Kummerow, C.D., 2014. An assessment of atmospheric water budget components over tropical oceans. Journal of climate 27, 2054–2071.

Chambers, J.Q., Artaxo, P., 2017. Deforestation size influences rainfall. Nature Climate Change 7, 175–176.

D'Almeida, C., Vörösmarty, C.J., Hurtt, G.C., Marengo, J.A., Dingman, S.L., Keim, B.D., 2007. The effects of deforestation on the hydrological cycle in amazonia: a review on scale and resolution. International Journal of Climatology: A Journal of the Royal Meteorological Society 27, 633–647.

Devaraju, N., Bala, G., Modak, A., 2015. Effects of large-scale deforestation on precipitation in the monsoon regions: Remote versus local effects. Proceedings of the National Academy of Sciences 112, 3257–3262.

Douville, H., Raghavan, K., Renwick, J., Allan, R., Arias, P., Barlow, M., Cerezo-Mota, R., Cherchi, A., Gan, T., Gergis, J., Jiang, D., Khan, A., Pokam Mba, W., Rosenfeld, D., Tierney, J., Zolina, O., 2021. Water Cycle Changes. Cambridge University Press, Cambridge, United Kingdom and New York, NY, USA. p. 1055–1210. doi:10.1017/9781009157896.010.

Drumond, A., Marengo, J., Ambrizzi, T., Nieto, R., Moreira, L., Gimeno, L., 2014. The role of the amazon basin moisture in the atmospheric branch of the hydrological cycle: a lagrangian analysis. Hydrology and Earth System Sciences 18, 2577–2598.

Duku, C., Hein, L., 2021. The impact of deforestation on rainfall in africa: a data-driven assessment. Environmental Research Letters 16, 064044.

Garcia-Carreras, L., Parker, D., 2011. How does local tropical deforestation affect rainfall? Geophysical Research Letters 38.

Gill, A.E., 1982. Atmosphere-ocean dynamics. volume 30. Academic press.

Hansen, M.C., Potapov, P.V., Moore, R., Hancher, M., Turubanova, S.A., Tyukavina, A., Thau, D., Stehman, S.V., Goetz, S.J., Loveland, T.R., et al., 2013. High-resolution global maps of 21st-century forest cover change. science 342, 850–853.

Hu, I.K., 2020. Exploring the Behavior of the Community Atmosphere Model in the Tropics: The Single-Column Root of a Hierarchy. Ph.D. thesis. University of Miami.

IPCC, 2022. Summary for Policymakers, in: Shukla, P., Skea, J., Slade, R., Khourdajie, A.A., van Diemen, R., McCollum, D., Pathak, M., Some, S., Vyas, P., Fradera, R., Belkacemi, M., Hasija, A., Lisboa, G., Luz, S., Malley, J. (Eds.), Climate Change 2022: Mitigation of Climate Change. Contribution of Working Group III to the Sixth Assessment Report of the Intergovernmental Panel on Climate Change. Cambridge University Press, Cambridge, UK and New York, NY, USA. doi:10.1017/9781009157926.001.

Lawrence, D., Vandecar, K., 2015. Effects of tropical deforestation on climate and agriculture. Nature climate change 5, 27–36.

Leite-Filho, A.T., Soares-Filho, B.S., Davis, J.L., Abrahão, G.M., Börner, J., 2021. Deforestation reduces rainfall and agricultural revenues in the brazilian amazon. Nature Communications 12, 1–7.

Lejeune, Q., Davin, E.L., Guillod, B.P., Seneviratne, S.I., 2015. Influence of amazonian deforestation on the future evolution of regional surface fluxes, circulation, surface temperature and precipitation. Climate Dynamics 44, 2769–2786.

Li, J.F., Xu, K.M., Richardson, M., Lee, W.L., Jiang, J.H., Yu, J.Y., Wang, Y.H., Fetzer, E., Wang, L.C., Stephens, G., et al., 2020. Annual and seasonal mean tropical and subtropical precipitation bias in cmip5 and cmip6 models. Environmental Research Letters 15, 124068.

Lin, J.L., 2007. The double-itcz problem in ipcc ar4 coupled gcms: Ocean–atmosphere feedback analysis. Journal of Climate 20, 4497–4525.

Makarieva, A., Gorshkov, V., 2009. Condensation-induced dynamic gas fluxes in a mixture of condensable and non-condensable gases. Physics Letters A 373, 2801–2804.

Makarieva, A.M., Gorshkov, V.G., 2007. Biotic pump of atmospheric moisture as driver of the hydrological cycle on land. Hydrology and earth system sciences 11, 1013–1033.

Makarieva, A.M., Gorshkov, V.G., Sheil, D., Nobre, A.D., Li, B.L., 2011. Where do winds come from? a new theory on how water vapor condensation influences atmospheric pressure and dynamics. URL: `https://acp.copernicus.org/articles/13/1039/2013/acp-13-1039-2013-discussion.html`.

Makarieva, A.M., Gorshkov, V.G., Sheil, D., Nobre, A.D., Li, B.L., 2013. Where do winds come from? a new theory on how water vapor condensation influences atmospheric pressure and dynamics. Atmospheric chemistry and Physics 13, 1039–1056.

Marengo, J.A., 2006. On the hydrological cycle of the amazon basin: A historical review and current state-of-the-art. Revista brasileira de meteorologia 21, 1–19.

Medvigy, D., Walko, R.L., Avissar, R., 2011. Effects of deforestation on spatiotemporal distributions of precipitation in south america. Journal of Climate 24, 2147–2163.

da Motta Paca, V.H., Espinoza-Dávalos, G.E., Moreira, D.M., Comair, G., 2020. Variability of trends in precipitation across the amazon river basin determined from the chirps precipitation product and from station records. Water 12, 1244.

Portmann, R., Beyerle, U., Davin, E., Fischer, E.M., De Hertog, S., Schemm, S., 2022. Global forestation and deforestation affect remote climate via adjusted atmosphere and ocean circulation. Nature communications 13, 1–11.

Sheil, D., 2018. Forests, atmospheric water and an uncertain future: the new biology of the global water cycle. Forest Ecosystems 5, 1–22.

Smith, C., Baker, J., Spracklen, D., 2023. Tropical deforestation causes large reductions in observed precipitation. Nature , 1–6.

Spengler, T., Egger, J., Garner, S.T., 2011. How does rain affect surface pressure in a one-dimensional framework? Journal of the atmospheric sciences 68, 347–360.

Spracklen, D., Baker, J., Garcia-Carreras, L., Marsham, J., 2018. The effects of tropical vegetation on rainfall. Annual Review of Environment and Resources 43, 193–218.

Spracklen, D., Garcia-Carreras, L., 2015. The impact of amazonian deforestation on amazon basin rainfall. Geophysical Research Letters 42, 9546–9552.

Stevens, B., 2005. Atmospheric moist convection. Annual Review of Earth and Planetary Sciences 33, 605–643.

Teuling, A.J., Taylor, C.M., Meirink, J.F., Melsen, L.A., Miralles, D.G., Van Heerwaarden, C.C., Vautard, R., Stegehuis, A.I., Nabuurs, G.J., de Arellano, J.V.G., 2017. Observational evidence for cloud cover enhancement over western european forests. Nature communications 8, 14065.

Tian, B., Dong, X., 2020. The double-itcz bias in cmip3, cmip5, and cmip6 models based on annual mean precipitation. Geophysical Research Letters 47, e2020GL087232.

Volodin, E.M., Mortikov, E.V., Kostrykin, S.V., Galin, V.Y., Lykossov, V.N., Gritsun, A.S., Diansky, N.A., Gusev, A.V., Iakovlev, N.G., Shestakova, A.A., et al., 2018. Simulation of the modern climate using the inm-cm48 climate model. Russian Journal of Numerical Analysis and Mathematical Modelling 33, 367–374.

Wang, J., Chagnon, F.J., Williams, E.R., Betts, A.K., Renno, N.O., Machado, L.A., Bisht, G., Knox, R., Bras, R.L., 2009. Impact of deforestation in the amazon basin on cloud climatology. Proceedings of the National Academy of Sciences 106, 3670–3674.

Wright, J.S., Fu, R., Worden, J.R., Chakraborty, S., Clinton, N.E., Risi, C., Sun, Y., Yin, L., 2017. Rainforest-initiated wet season onset over the southern amazon. Proceedings of the National Academy of Sciences 114, 8481–8486.

Xu, R., Li, Y., Teuling, A.J., Zhao, L., Spracklen, D.V., Garcia-Carreras, L., Meier, R., Chen, L., Zheng, Y., Lin, H., et al., 2022. Contrasting impacts of forests on cloud cover based on satellite observations. Nature communications 13, 670.

Zhang, G.J., Song, X., Wang, Y., 2019. The double itcz syndrome in gcms: A coupled feedback problem among convection, clouds, atmospheric and ocean circulations. Atmospheric Research 229, 255–268.

Zhang, X., Liu, H., Zhang, M., 2015. Double itcz in coupled ocean-atmosphere models: From cmip3 to cmip5. Geophysical Research Letters 42, 8651–8659.

# A | Additional figures

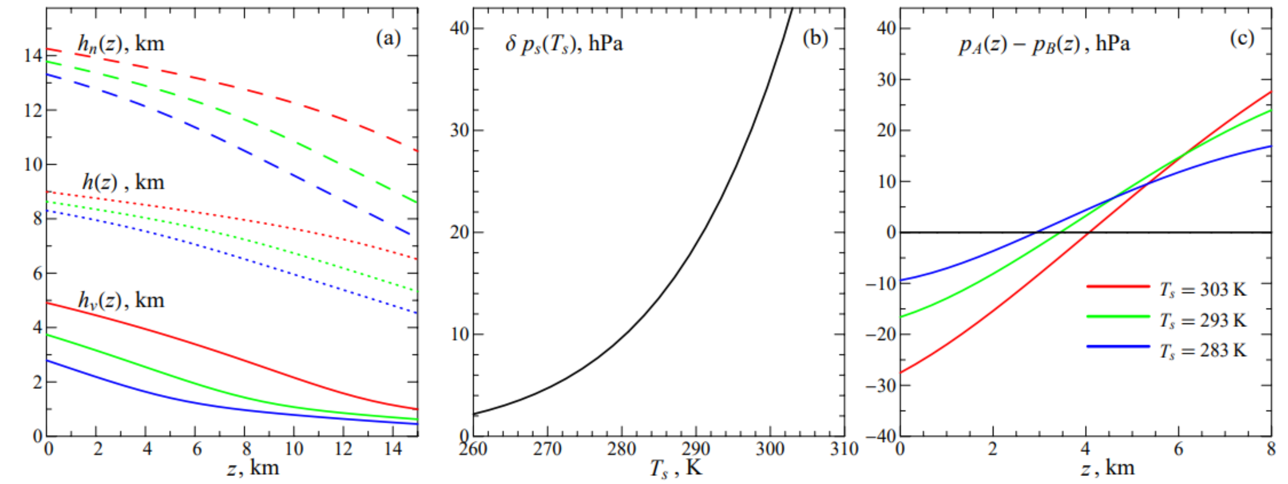


Figure A.1: *This figure is taken from Makarieva et al. (2013) to compare to the replica study. Original caption: "(a) Scale height of saturated water vapor $h_v(z)$ (Eq. 24), hydrostatic scale height of water vapor $h_n(z)$ (Eq. 26), and scale height of moist air $h(z)$ (Eq. 20) in the column with moist adiabatic lapse rate (Eq. 22) for three values of surface temperature $T_s$; (b) condensation-induced drop of air pressure at the surface (Eq. 27) as dependent on surface temperature $T_s$; (c) pressure difference versus altitude z between atmospheric columns A and B with moist and dry adiabatic lapse rates, Eqs. (30) and (31), respectively, for three values of surface temperature $T_s$. Height $z_c$ at which $P_A(z_c) - P_B(z_c) = 0$ is 2.9, 3.4 and 4.1 km for 283, 293 and 303 K, respectively. Due to condensation, at altitudes below $z_c$ the air pressure is lower in column A despite it being warmer than column B."*

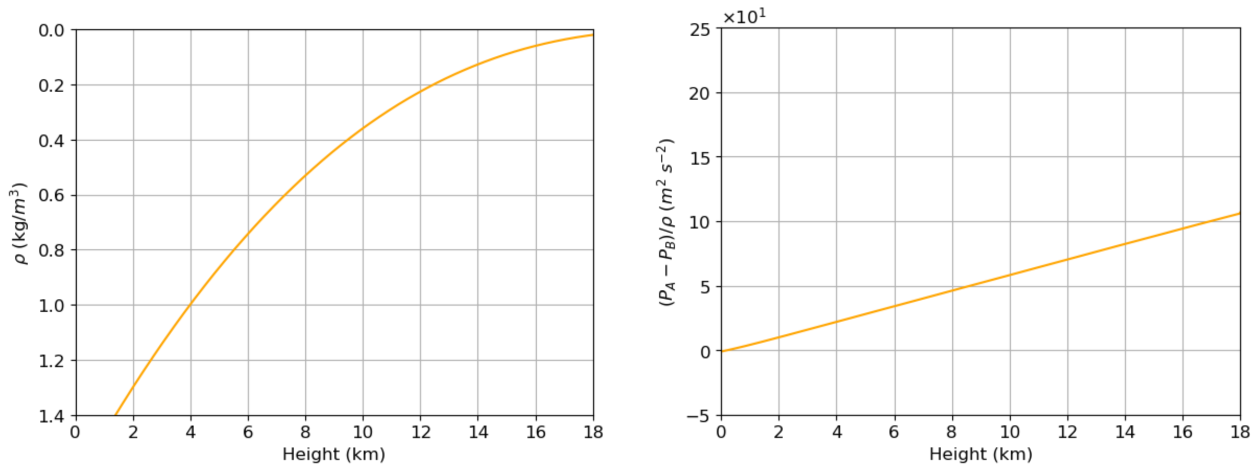


(a) (b)

Figure A.2: Subfigure (a) shows the density profiles for the initial surface temperatures of 214 K, which is needed to condense 0.2 $kg/m^2$ of water vapor in the adjusted condensation experiment by Makarieva et al. (2013). Subfigure (b) shows the pressure difference (left subfigure in figure 3.4) divided by the density, which is used in this research as a proxy for the pressure gradient force.